

# ANTENNA DESIGN FOR MICROWAVE DIGITAL COMMUNICATIONS

**T.C. YÜKSEKÖĞRETİM KURULU  
DOKÜMANTASYON MERKEZİ**

A Thesis Submitted to the  
Graduate School of Natural and Applied Sciences of  
Dokuz Eylül University  
In Partial Fulfillment of the Requirements for  
the Degree of Master of Science in Electrical and Electronics Engineering

109680

by

Özgür TAMER

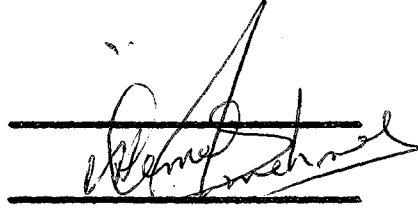
109680

July, 2001

İZMİR

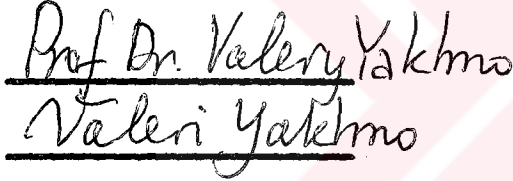
## M.Sc. THESIS EXAMINATION RESULT FORM

We certify that we have read this thesis, entitled "Antenna design for Microwave Digital Communications" completed by Özgür TAMER under supervision of Prof. Dr. Kemal Özmehtmet and that in our opinion it is fully adequate, in scope and in quality, as a thesis for the degree of Master of Science.

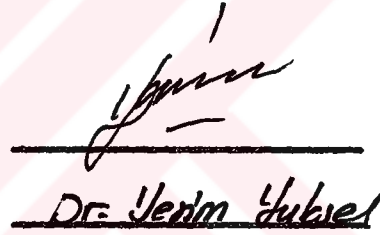


T.C. YÜKSEKÖĞRETİM KURULU  
DOKÜMANTASYON MERKEZİ

Prof. Dr. Kemal ÖZMEHMET  
(Advisor)

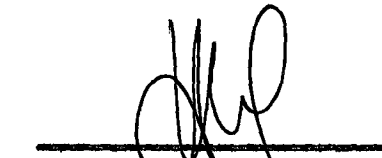


(Committee Member)



(Committee Member)

Approved by the  
Graduate School of Natural and Applied Sciences



Prof. Dr. Cahit HELVACI  
Director

## ACKNOWLEDGEMENTS

First of all I am grateful to my advisor Prof. Dr. Kemal ÖZMEHMET for his never ending support and invaluable guidance with his deep and esteemed experience.

I also benefited from guidance and support of academic personnel of Electrical and Electronics Engineering Department of Dokuz Eylül University.

My family and my sweetheart Sibel always encouraged me to finalize this work. I want to thank them for their endless support.

Since this is a thesis including practical work I would have limited ability without substrate support of GIL Technologies and discrete semiconductor support of On Semiconductors. I want to thank them for their support on educational institutions.

---

## ABSTRACT

---

In this thesis a suitable antenna design to operate in a microwave digital communication system is aimed. Microwave digital communications is widely used in land mobile satellite communications which becomes a good area of operation for us.

In order to achieve this aim aperture coupled microstrip phased array antenna is chosen. Antenna is controlled with two DC voltage sources. Antenna beam is to be directed in 90 degrees range for tracking all visible satellites. Aperture coupling will give us plenty of space to place phase shifting circuitry.

## ÖZET

Bu tez çalışması ile sayısal mikrodalga haberleşme sistemleri ile kullanılmak üzere bir anten tasarımı amaçlanmıştır. Sayısal mikrodalga sistemler yaygın olarak gezgin uydu haberleşme sistemlerinde kullanıldığı için anten tasarımı bu alanda kullanılabilir şekilde yapılmıştır.

Bu tasarımı gerçekleştirmek amacıyla boşluk beslemeli fazlı mikroşerit dizi anten kullanılmıştır. Anten fazı DA voltaj kaynağı ile kontrol edilmekte böylece anten maksimum ışınması istenen yöne çevrilebilmektedir. Anten maksimum ışınmasının gökyüzünde 90 derecelik bir alanı taraması düşünülmektedir. Bu sayede gökyüzünde haberleşmeye uygun bütün uydular bulunulabilecektir.

---

# CONTENTS

---

	Pages
Contents .....	VI
List of Tables .....	VIII
List of Figures.....	XI

## Chapter One INTRODUCTION

1.1 Antennas for Land Mobile Satellite Systems .....	1
1.2 Main Idea .....	2
1.3 The Aim Of The Thesis .....	4
1.4 Outline Of The Thesis .....	5

## Chapter Two THEORETICAL BACKGROUND

2.1 Microstrip Antennas .....	6
2.1.1 Transmission Line Model of a MSA.....	8
2.1.2 Cavity Model.....	9
2.1.2.1 Radiation of Rectangular MSA Using Cavity Modeling .....	12
2.1.2.2 Cavity Model For Circular Patch Antennas .....	14
2.1.3 Feeding Methods of MSA .....	15
2.1.3.1 Aperture Coupled Feeding of MSA .....	17
2.1.3.2 Applying Cavity Model to Aperture Coupled MSA .....	19

2.2	Phased Array Theory .....	21
2.2.1	Antenna Arrays .....	21
2.2.2	Planar Array .....	22
2.2.3	Circular Array.....	23
2.2.4	Phased Array Theory .....	24
2.3	Phase shifter Design .....	28

### Chapter Three

#### DESIGN AND IMPLEMENTATION

3.1	Design Of An Aperture Coupled Circular MSA at 1500 MHz .....	31
3.1.1	Design Of A Circular Parch .....	31
3.1.2	Aperture Coupled Ceeding.....	35
3.2	Two Antenna Aperture Coupled Microstrip Array Design .....	38
3.3	Phase Shifter Design.....	43
3.4	Phased Array Antenna Design.....	50

### Chapter Four

#### CONCLUSION AND FUTUREWORK

4.1	Discussion on Antenna Performance.....	507
4.2	Futurework.....	509
<b>REFERENCES .....</b>		<b>60</b>
<b>APPENDIX A.....</b>		<b>62</b>

## LIST OF FIGURES

---

	<b>Page</b>
Figure 1-1 Multi satellite communication system.....	2
Figure 1-2 Microstrip Antenna .....	3
Figure 2-1 Rectangular Microstrip Antenna .....	6
Figure 2.2 Microstrip antenna .....	8
Figure 2-3 Cavity model of a MSA .....	9
Figure 2-4 Electric field distribution of a rectangular MSA .....	10
Figure 2-5 simplified circuit model of a MSA.....	11
Figure 2-6 Radiation model of MSA .....	12
Figure 2-7 E and H field patterns of a MSA .....	13
Figure 2-8 3D radiation pattern for rectangular MSA .....	14
Figure 2-9 Feeding techniques of MSA (a),(b) coaxial feeding (c) microstrip feeding .....	15
Figure 2-10 Proximity Coupled Feeding Technique.....	17
Figure 2-11 Aperture coupled feeding technique .....	17
Figure 2-12 Boundary conditions at an aperture fed by a microstrip line .....	19
Figure 2-13 Aperture coupling configuration .....	20
Figure 2-14 A uniform linear array.....	21
Figure 2-15 Planar array .....	22
Figure 2-16 Circular Array Configuration .....	24
Figure 2-17 Linear Phased array antenna feed currents.....	25
Figure 2-18 Phase shifts of (a)0° (b)45° (c)90° (d) 180° applied to a 2 antenna array .....	25
Figure 2-19 Scheme of a Phased Array antenna .....	27
Figure 2-20 3 phase level digital phase shifter .....	28
Figure 2-21 Analog phase shifter with a circulator.....	29



Figure 3-1 H plane polar plot diagram of the aperture coupled circular MSA (substrate is epoxy) .....	33
Figure 3-2 E plane polar plot diagram of the aperture coupled circular MSA (substrate is epoxy) .....	33
Figure 3-2 Frequency Response of the three antennas. (Continuous line transparent plexiglas, dotted line epoxy, long dotted line is white plexiglas) .....	34
Figure 3-3 Return Loss analysis of three different materials.....	34
(continuous line is epoxy, small dotted is white plexiglas and long dotted line is the transparent plexiglas) .....	34
Figure 3-3 aperture coupled feeding illustration.....	36
Figure 3-4 Return Loss measurement system with Spectrum Analyzer .....	37
Figure 3-5 Illustration of a two antenna array with $d = \lambda_0/2$ and 0 degree phase difference between them. ....	39
Figure 3-6 Dual array antenna feed for aperture coupled feed MSA array .....	39
Figure 3-7 Power divider on the feed layer.....	39
Figure 3-8 Wilkinson power divider.....	40
Figure 3-9 Dual antenna array return loss graphics of dual array.....	41
Figure 3-10 Frequency Response of dual array .....	41
Figure 3-11 Polar plot of E field radiation pattern of dual array antenna .....	42
Figure 3-12 Polar plot of H field radiation pattern of dual array antenna.....	42
Figure 3-15 Loaded Line Phase Shifter .....	43
Figure 3-16 Simulation Screen Capture of Simulation at APLAC.....	44
Figure 3-17 Impedance Behavior of an open circuited transmission line.....	45
Figure 3-18 Magnitude and phase response of a Loaded line phase shifter. ....	46
Figure 3-19 Phase Shift of the simulation circuitry at a specified frequency .....	47
Dotted line $V_b=1V$ Squared marked line $V_b=5V$ 47 Cross marked line $V_b=10V$ Small dotted line $V_b=15 V$ 47 Square + dotted line $V_b=20 V$ Scratch marked line $V_b=25 V$ 47 Continuous line $V_b=30 V$ .....	47
Figure 3-20 Printed circuit diagram of the phase shifter .....	47
Figure 3-21 Feed layer with phase shifters for aperture coupled dual array MSA... ..	50
Figure 3-22 Effect of changing silver colored phase shifter voltage. ....	51
Figure 3-22 Effect of changing red colored phase shifter voltage. ....	51

Figure 3-23 Frequency response of the phase array antenna .....	52
Figure 3-24 Radiation pattern of the phased array antenna with $V_{bs}=16.5V$ $V_{bn}=16V$ .....	53
Figure 3-25 Radiation pattern of the phased array antenna with $V_{bs}=19V$ $V_{bn}=16V$ .....	53
Figure 3-26 Radiation pattern of the phased array antenna with $V_{bs}=25V$ $V_{bn}=16V$ .....	54
Figure 3-27 Radiation pattern of the phased array antenna with $V_{bs}=16V$ $V_{bn}=22V$ .....	54
Figure 3-28 Radiation pattern of the phased array antenna with $V_{bs}=16V$ $V_{bn}=24V$ .....	55
Figure 3-29 Radiation pattern of the phased array antenna with $V_{bs}=16V$ $V_{bn}=27V$ .....	55



---

## LIST OF TABLES

---

	<b>Pages</b>
Table 2-1 Application areas of MSA .....	7
Table 2-2 Properties Effected by Layers.....	27
Table 3-1 Available Substrates Properties .....	32
Table 3-3 Return Loss Comparison of aperture size on GML1000.....	38
Table 3-3 Performance test of the loaded line phase shifter.....	49



---

## CHAPTER ONE

# INTRODUCTION

---

Reliable and high capacity communication networks is gaining more importance in recent years. Wireless communications is an important field in high performance communications since it is very flexible and it permits mobility. In case of wireless communication we should use higher (in other words microwave or millimeterwave) frequencies for wider bandwidths, thus for fast and high capacity networks.

Frequency band is not the only criteria because wireless media is a noisy media which can cause loss of information. Solution for this problem is digital communications. Because digital communications has the ability to be reconstructed with various methods. Thus a solution for today's communication needs is Microwave Digital Communications.

### **1.1 Antennas for Land Mobile Satellite Systems**

Microwave digital communications are widely used for the land mobile satellite systems (LMSS) in recent years since a very reliable system is required because of the very long distance and nonhomogenous environmental effects and variable atmospheric conditions.

Mobile station antennas for LMSS must be capable of communicating with all visible satellites because of not only the unit is moving but also the satellite is moving as can be seen in Figure 1.1. This brings out the roaming case for even a stationary unit. Thus a mobile unit must continue communicating with the next satellite in view when it is out of range of the communicated satellite. So in a multi-satellite communication network we need the ability to switch communication to neighbouring satellites. An antenna with a very wide beamwidth can be a suitable design criteria for such need which is also a generally preferred technology in today's

mobile devices.

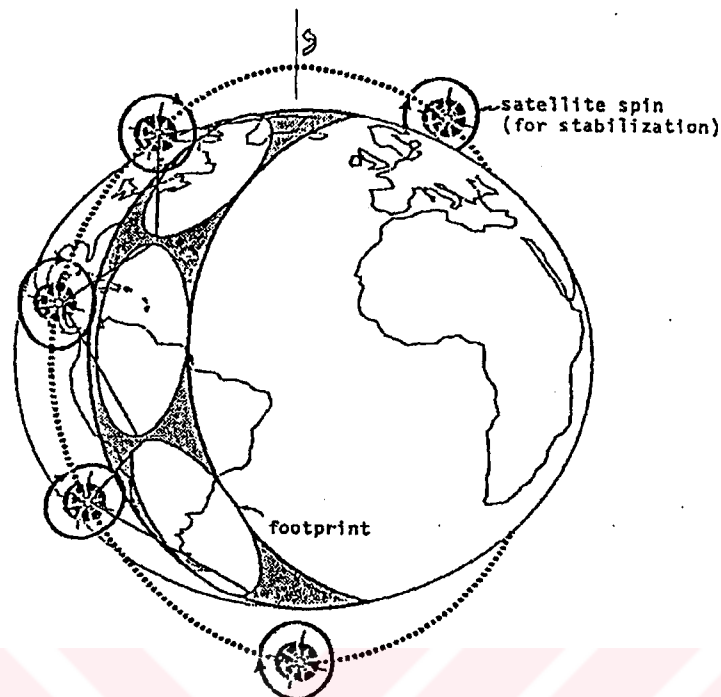


Figure 1-1 Multi satellite communication system

But such an antenna would have a very low gain. Thus we must have a device which transmits much more RF power in order to communicate with the satellite or it should receive a very weak signal. In each case this procedure consumes more energy which is a very critical case for mobile applications.

Another important criteria for a LMSS antenna is its small profile due to decrease its effect on mobility of the person carrying the unit or vehicle which it is mounted on.

## 1.2 Main Idea

In this thesis it is aimed to design a high gain, low profile antenna to be used as a mobile unit antenna for LMSS systems.

A high gain antenna with a very narrow beam can be used. This narrow beam can locate and communicate with the neighbouring satellites by tracking the whole sky.

This can be accomplished by using a phased array antenna. Phased array is a technique which enables us to steer the main beam of the array to any point in the

sky by controlling the phase difference between antennas in the array. This phenomenon can be analyzed for a linear array by using the following

$$AF = \frac{1}{N} \left| \frac{\sin\left(\frac{N\psi}{2}\right)}{\sin\left(\frac{\psi}{2}\right)} \right| \quad (1.1)$$

Where  $\psi = k \cdot d \cdot \cos \theta + \beta$  (1.2)

Here  $\beta$  denotes the phase angle between the antenna elements,  $N$  is the number of antennas in the array  $k$  is the propagation factor and  $d$  is the distance between antennas. It can be seen that array factor changes with changing  $\beta$ . This phenomenon is explained in more detail in Chapter 2. Antenna radiation pattern is obtained by multiplying array factor with element factor, which is radiation characteristic of each element. Thus when we change the phase angle between antennas we can change the direction of radiation and steer the main beam of the array antenna. Major advantage of this technique is that, it is very fast and it does not occupy more space than the antenna itself.

Microstrip antennas are low profile antennas which are widely preferred in vehicular communication technologies. They are also very suitable for phased array applications because of easy integrability to printed circuit boards.

Basic configuration of a MSA is a metallic patch printed on a relatively thin, grounded dielectric substrate. This can be seen from the Figure 1.2.

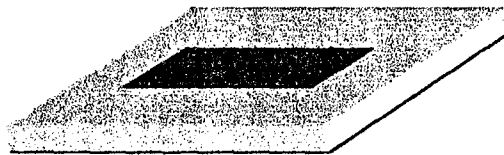


**Figure 1.2 Microstrip Antenna**

There are two main disadvantages for MSA's when used in high performance microwave digital communications. These antennas have small bandwidth and low gain but since we will use an array antenna consisting of microstrip antenna elements we can increase gain by using a suitable array topology.

We can also increase the bandwidth of a microstrip antenna by using considerably

thick and low dielectric material (2-3mm thickness with  $\epsilon_r=2-3$ ). Since this kind of material is not suitable for microstrip feeds we should separate feed and patch layers by using aperture coupled feeding.

### 1.3 The Aim Of The Thesis

Goal of this thesis is to design a high gain phased array antenna to be used in LMSS systems. It is to be obtained by a aperture coupled fed microstrip phased array antenna with analog control of the phase shift.

Three main objectives can be defined for this thesis are as follows;

*i) Design of an aperture coupled microstrip antenna*

Aperture coupling will be used to feed microstrip antenna in order to separate feed layer and antenna layer. We can eliminate unwanted radiation of microstrip feed line and increase bandwidth of the MSA

*ii) Design of a high gain microstrip array antenna*

A microstrip array antenna design is under consideration to fit needs of a LMSS. Aperture coupled feeding technique will be used for the array feed also.

*iii) Design of an analog phase shifter*

A phase shifter is to be designed to control relative phase difference between microstrip antenna elements. This control will be done with a loaded line phase shifter circuitry (Garver 1976) with analog control of the varicap reverse voltage.

As a final work results from these design works will be combined in order to build up an aperture coupled phased array antenna.

#### **1.4 Outline Of The Thesis**

Following chapters of this thesis is organized as follows;

In Chapter 2 theoretical background for thesis work is given. Microstrip antenna is defined and radiation , impedance modelling of such an antenna is done. Array theory followed by phased array concept is given. And phase shifter circuitries are explained.

In Chapter 3 step by step design is explained and practical results of the designs were given. First design of an aperture coupled microstrip antenna is explained and then practical results of the implemented circuit is given. Then a dual array antenna design is explained. Results of such an array is given followed by. At next step a phase shifter is implemented on the array to construct a phased array antenna and practical results are discussed for it.

Chapter 4 is where the conclusion is made and futureworks are defined for this thesis work.



---

## CHAPTER TWO

# THEORETICAL BACKGROUND

---

### 2.1 Microstrip Antennas

A microstrip antenna (MSA) can be described as two parallel conducting layers separated by a single thin dielectric substrate. Wider conductor is called the ground plane and the smaller conductor is the radiating patch antenna. Radiating patch can be in various shapes most common types are rectangular and circular patch. Patch conductor is designed in order to resonate at specified frequency (Figure 2.1).

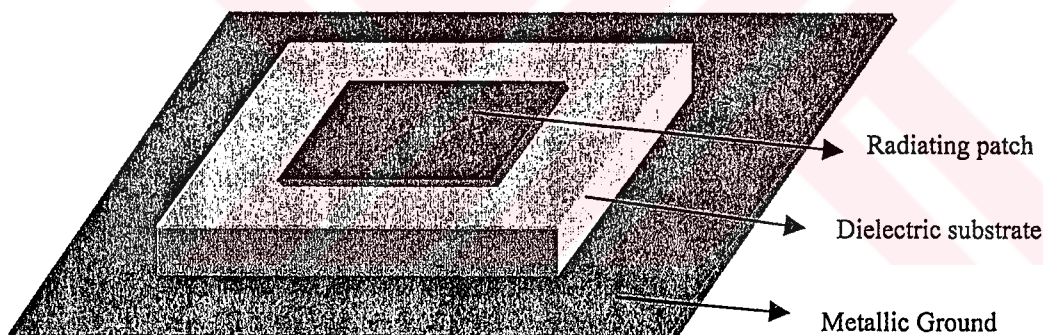


**Figure 2-1 Rectangular Microstrip Antenna**

Practical frequency range for microstrip antennas is from 400 MHz to 60 GHz. This range is determined by dimension of the patch.

Typical advantages of microstrip antennas are their low profile, low weight, low cost, easy integrability to arrays or with microwave integrated circuits or polarization diversity. Major application areas are shown in Table 2-1 (Pozar 1992).

Some disadvantages of MSA are their narrow bandwidth, spurious feed radiation, poor polarization purity, limited power capacity and tolerance problems. But these are mostly overcome with different feeding techniques and patch types developed in recent years.

**Table 2-1 Application areas of MSA**

<b>Platform</b>	<b>Systems</b>
Aircraft	<i>Radar, Communication, Navigation, Altimeter, Landing Systems</i>
Missiles	<i>Radar, Fuzing, Telemetry</i>
Satellites	<i>Communications, TV Broadcast, remote sensing and radiometer</i>
Ships	<i>Communications, radar, navigation</i>
Land Vehicles	<i>Mobile satellite phone, mobile radio</i>
Other	<i>Biomedical systems, intruder alarms</i>

Substrate thickness and dielectricity is the most important parameters of a MSA. When substrate gets thinner the current on the patch element is in very close proximity to its negative image caused by the presence of the ground layer. This cancels of near radiated fields and more energy is stored in the substrate. This effect can also be observed by changing the substrate dielectricity. If we increase dielectricity more energy is bounded inside the feed substrate.

Antennas require loosely bounded fields for better radiation into space. This is just the opposite case for a microstrip transmission line substrate because tightly bounded fields are required for less radiation loss (Pojar 1992)

Layer dielectric constant does not only effect antennas efficiency but also effects radiation frequency of the antenna, because antennas resonance frequency depends on wavelength inside the dielectric media  $\lambda_g$  and wavelength is a function of dielectric constant;

$$\lambda_g = \frac{\lambda_0}{\sqrt{\epsilon_r}} \quad (2.1)$$

When a MSA is operating in transmitting mode antenna is driven with a voltage between the feed line and the ground plane. This excites a current on the patch, and a vertical electric field occurs between the patch and the ground plane.

Radiation of MSAs can be modeled in many ways. Two very basic models are transmission line modeling and cavity modeling of MSA. These models are

relatively simple because they involve several simplifying approximations. They are easy to use and can provide useful information on antenna patterns, impedance, efficiency, and bandwidth.

### 2.1.1 Transmission Line Model of a MSA.

In transmission line modeling of MSA patch is modeled as two parallel radiating slots. Each radiating edge of length  $a$  is modeled as a narrow slot radiating into a half space with a slot admittance given by;

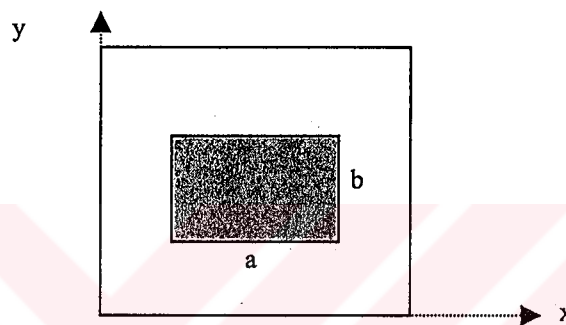


**Figure 2-2 Microstrip antenna**

$$G_1 + jB_1 = \frac{\pi a}{\lambda_0 z_0} [1 + j(1 - 0.636 \ln k_0 w)] \quad (2.2)$$

Where  $\eta_0$  and  $k_0$  denotes characteristic impedance propagation factor of free space respectively and given by;

$$\eta_0 = \sqrt{\frac{\mu_0}{\epsilon_0}} \quad k_0 = \frac{2\pi}{\lambda_0} \quad (2.3)$$

Here  $w$  is the slot width of the antenna and is equal to the substrate thickness ( $t$ ).

Thus the characteristic admittance of the slot is given by

$$Y_0 = \frac{a\sqrt{\epsilon_r}}{t\eta_0} \quad (2.4)$$

In order to excite slots  $180^\circ$  out of phase  $b$  is set to slightly less than  $\lambda/2$ . This adjustment brings out that admittance of the second slot ;

$$G_2 + jB_2 = G_1 - jB_1 \quad (2.5)$$

So that total input impedance becomes

$$Y_{in} = 2G_1 \quad (2.6)$$

For  $a=\lambda_0/2$   $G_1$  becomes 0.00417 mho ;  $R_{in}=120 \Omega$  and resonant frequency is;

$$f_r = \frac{c}{\lambda_0 \sqrt{\epsilon_{eff}}} \quad (2.7)$$

Even if this model gives good results it can be used only for rectangular patches (Balanis 1996).

### 2.1.2 Cavity Model

In cavity modelling of a MSA patch is viewed as a thin TMz mode cavity with magnetic walls.

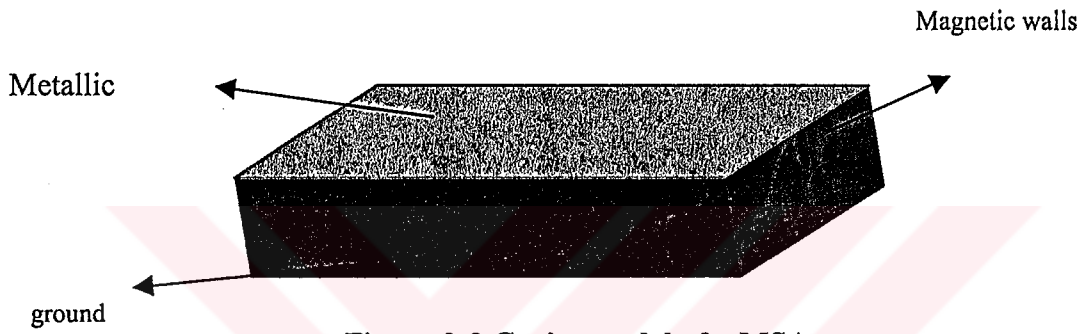


Figure 2-3 Cavity model of a MSA

Field between the patch and the ground plane is expanded in terms of a series of cavity resonant modes with resonant frequencies associated with each mode. These calculations are made according to matrix equations where resonant modes are calculated as eigenfunctions with eigenvalues of resonant frequencies.

Electric field inside this cavity is given by the following equation;

$$E_z(x, y) = \sum_m \sum_n A_{mn} e_{mn}(x, y) \quad (2.8)$$

Where  $A_{mn}$  are the amplitude coefficients of mode  $mn$  and  $e_{mn}$  are the  $z$  directed orthonormal field vectors. If the walls are assumed to have no fringing (perfect open circuit case) no radiation occurs and following equation are valid.

$$e_{mn}(xy) = \frac{X_{mn}}{\sqrt{\epsilon a b t}} \cos k_n x \cos k_m y \quad (2.9)$$

here;

$$k_{mn}^2 = \omega_{mn}^2 \mu \epsilon = k_n^2 + k_m^2 \quad (2.10)$$

$k_n$  and  $k_m$  are given for the non radiating cavity as;  $k_n = n\pi/a$  and  $k_m = m\pi/b$

Thus tangential of the cavity is zero. If we let walls to fringe thus radiation occurs magnetic vector field equation is effected.

If fringing occurs at perimeter walls , magnetic field component on non radiating magnetic walls is no longer zero. Thus losses occur. These losses are namely substrate loss, copper loss, and radiation. In cavity model radiation is modeled as loss.

Amplitude coefficients in this case are given as;

$$A_{mn} = jI_0 \sqrt{\frac{\mu t}{ab}} \frac{kX_{mn}}{k^2 - k_{mn}^2} G_{mn} \cos(k_m y_0) \cos(k_n x_0) \quad (2.11)$$

Where  $x_0$  and  $y_0$  are the feed point coordinates and  $G_{mn}$  accounts for the area of the feed point.

Electric field can be evaluated from the above equations as;

$$G_{mn} = \frac{\sin\left(\frac{n\pi d_x}{2a}\right) \sin\left(\frac{m\pi d_y}{2b}\right)}{\frac{n\pi d_x}{2a} \frac{m\pi d_y}{2b}} \quad (2.12)$$

Here  $d_x$  and  $d_y$  denotes distance of feed line position to origin.

$$E_z(x, y) = jI_0 Z_0 k \sum_{m=0}^{\infty} \sum_{n=0}^{\infty} \frac{\psi_{mn}(x, y) \psi_{mn}(x_0, y_0)}{k^2 - k_{mn}^2} G_{mn} \quad (2.13)$$

Where

$$\psi_{mn} = \frac{X_{mn}}{\sqrt{ab}} \cos \frac{n\pi x}{a} \cos \frac{m\pi y}{b} \quad (2.14)$$

We can see the electric field distribution on a microstrip line fed MSA on Figure2.4.

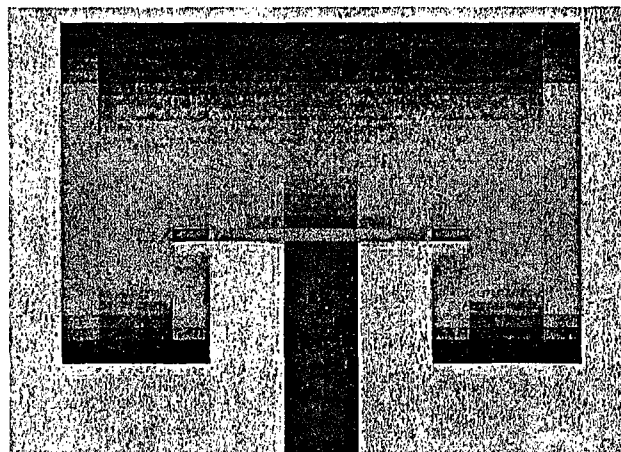


Figure 2-4 Electric field distribution of a rectangular MSA

The voltage at the feed point can be computed as

$$V_{in} = -tE_z(x_0, y_0) \quad (2.15)$$

Therefore input impedance can be calculated as;

$$Z_{in} = \frac{V_{in}}{I_0} = -jZ_0 kt \sum_{m=0}^{\infty} \sum_{n=0}^{\infty} \frac{\psi_{mn}^2(x_0, y_0)}{k^2 - k_{mn}^2} G_{mn} \quad (2.16)$$

The (0,0) term indicates the substrate loss

The (1,0) mode denotes the dominant RF mode radiation. If patch is square (0,1) mode represents a degenerate radiation mode also. A simplified equivalent model can be seen in Figure 2-5

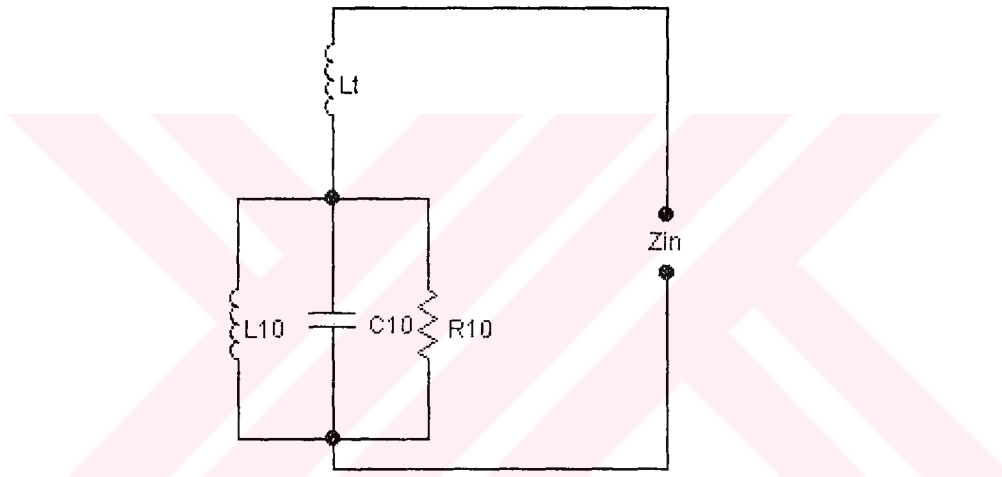


**Figure 2-5 simplified circuit model of a MSA**

Here  $L_t$  denotes all other modes than (1,0) mode. We can denote  $Z_{in}$  as

$$Z_{in} = jX_L - \frac{j(\omega / C_{10})}{\omega^2 - (\omega_r + j\omega_i)^2} \quad (2.17)$$

Where we can obtain  $C_{10}$  and  $(\omega_r + j\omega_i)^2$  by ;

$$C_{10} = \frac{1}{2} C_{dc} \cos^{-2}(\pi y_0 / b) \quad (2.18)$$

$$(\omega_r + j\omega_i)^2 = \omega_{10}^2 (1 + j/Q) \quad (2.19)$$

We can obtain the propagation constant for the dominant propagation mode (1,0) as;

$$\tan k_{10} b = \frac{2 k_{10} \alpha_{10}}{k_{10}^2 - \alpha_{10}^2} \quad (2.20)$$

Where

$$\alpha_{10} = j \frac{1\pi Z_0 t}{\lambda_0 a} Y_w \quad (2.21)$$

Here  $Y_w$  is the admittance of the radiating walls and  $Z_0$  is the characteristic impedance of the feed line. Thus radiation resistance can be calculated by using;

$$R_{rad} = \frac{Q_r}{\omega C_{10}} \quad (2.22)$$

Where  $Q_r$  is the radiation quality factor and can be calculated using

$$Q_r = \frac{\text{Re}(k_{10})}{2 \text{Im}(k_{10})} \quad (2.23)$$

As stated above in addition to radiation losses caused by radiation resistance, substrate losses ( $G_{di}$ ) and copper losses ( $G_{cu}$ ) occur which effects our antennas radiation efficiency. We can calculate the total conductance as;

$$G_{in} = G_{rad} + G_{cu} + G_{di} = \frac{1}{R_{rad}} + G_{cu} + G_{di} \quad (2.24)$$

Efficiency of the antenna can be calculated by ;

$$\eta = \frac{G_{rad}}{G_{in}} \quad (2.25)$$

Which ranges from 95 to 99 for a typical MSA (Carver 1981).

### 2.1.2.1 Radiation Of Rectangular MSA Using Cavity Modeling

The far field radiation pattern of a rectangular MSA can be calculated by modeling the radiator as two parallel uniform magnitude line sources of length  $a$ , separated by distance  $b$  or as two equivalent electric current sources as in Figure 2.6

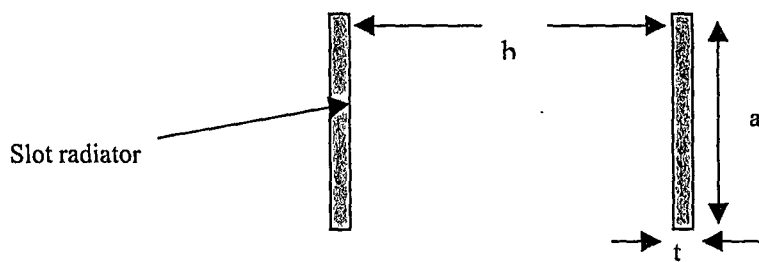


**Figure 2-6 Radiation model of rectangular MSA**

The effect of the ground plane and substrate is handled by imaging the slot at an electrical distance  $k_t$ .

If the slot voltage across either radiating edge is taken as  $V_0$  the evaluated equations for fields are;

$$E_{\theta} = -\frac{jV_0 k_0 a e^{-jk_0 r}}{\pi r} [\cos(kt \cos \theta)] \left[ \frac{\sin \left[ k_0 \frac{a}{2} \sin \theta \sin \phi \right]}{k_0 \frac{a}{2} \sin \theta \sin \phi} \right] \left[ \cos \left( k_0 \frac{b}{2} \sin \theta \cos \phi \right) \right] \cos \phi \quad (2.26)$$

$$E_{\phi} = \frac{jV_0 k_0 a e^{-jk_0 r}}{\pi r} [\cos(kt \cos \theta)] \left[ \frac{\sin \left[ k_0 \frac{a}{2} \sin \theta \sin \phi \right]}{k_0 \frac{a}{2} \sin \theta \sin \phi} \right] \left[ \cos \left( k_0 \frac{b}{2} \sin \theta \cos \phi \right) \right] \cos \phi \sin \phi \quad (2.27)$$

$$0 \leq \theta \leq \pi/2$$

Here  $\theta$  and  $\phi$  denotes spherical coordinates and propagation constant  $k$  inside the dielectric media is given by ;

$$k = k_0 \sqrt{\epsilon_r} \quad (2.28)$$

Image factor for the above fields is  $\cos(k t \cos \theta)$  and it is obtained by assuming that the slot is imbedded in a half space of dielectric constant  $\epsilon_r$ . Resulting radiation pattern can be seen in Figure 2-4 and 2-5.

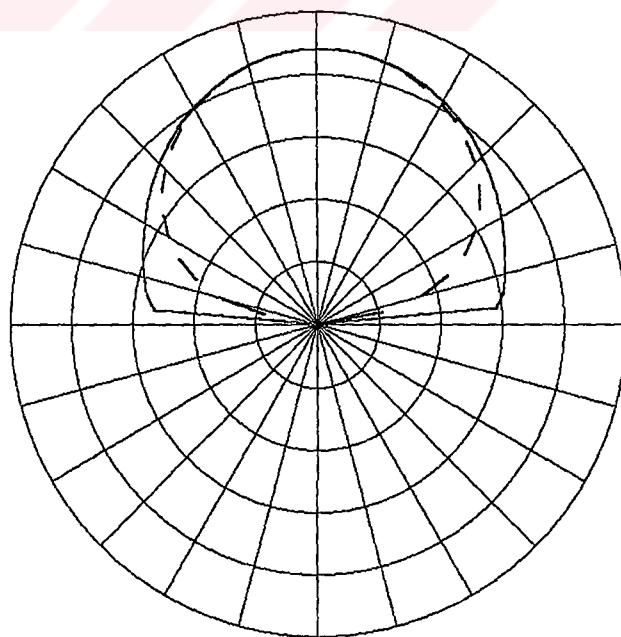
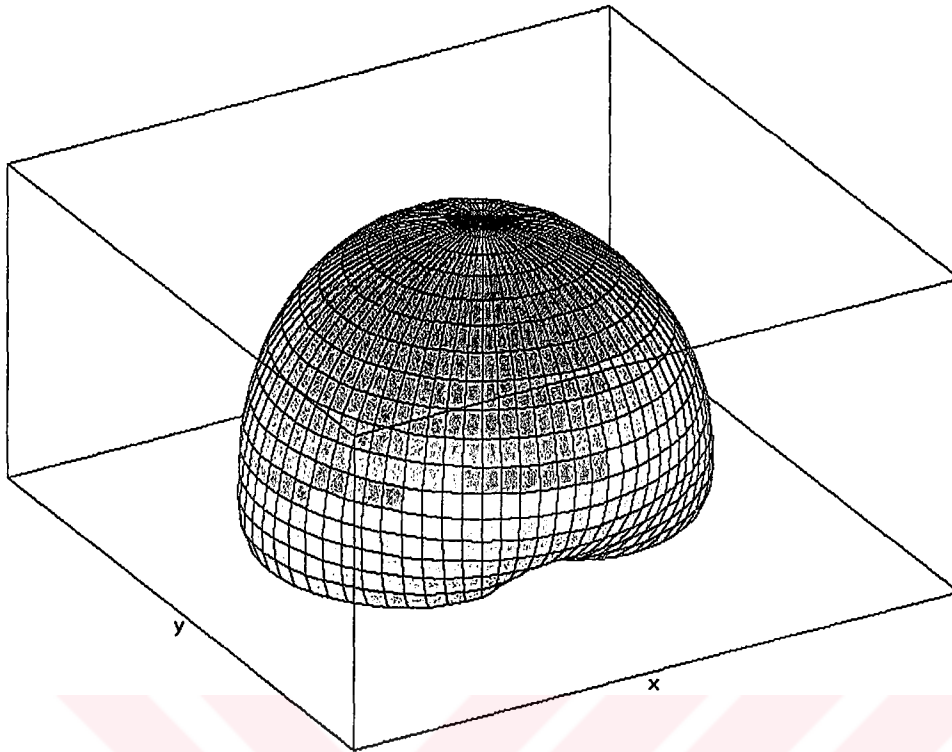


Figure 2-7 E and H field patterns of a MSA  $E_{\phi}$  dotted  $E_{\theta}$  continuous line  
( $\phi=135$ )





**Figure 2-8 3D radiation pattern for rectangular MSA**

If we numerically calculate directivity from above equations we can see that thickness is inversely proportional to antenna directivity. (Carver 1981)

#### 2.1.2.2 Cavity Model for Circular Patch Antennas

The modes that are supported by a circular MSA are  $TM^z$  modes while z axis is perpendicular to the antenna. In a circular patch antenna only dimension under control is the radius of the patch. By changing it we do not change the order of the modes but change the resonant frequency of the antenna.

For Cavity modeling we assume a cylindrical perfect magnetic conductor around the circular periphery of the cavity with two electric conductors surrounding it.

For  $TM^z$  mode magnetic vector potential  $A_z$  must satisfy the homogenous wave equation;

$$\nabla^2 A_z(\theta, \phi, z) + k^2 A_z(\theta, \phi, z) = 0 \quad (2.29)$$

By applying boundary conditions at perfect magnetic and electric conductors we evaluate the equation.

$$A_z = B_{mnp} J_m(k_\rho \rho') [A_z \cos(m\phi') + B_z \sin(m\phi')] \cos(k_z z') \quad (2.30)$$

with the equation

$$k_p^2 + k_z^2 = k_r^2 = \omega_r^2 \mu \epsilon \quad (2.31)$$

where  $\theta', \phi', z'$  represent coordinates inside the cavity and  $J_m(x)$  represent the Bessel function of the first kind of order  $m$ .

$$k_\theta = \frac{X'_{mn}}{a} \quad (2.32)$$

$$k_z = \frac{\theta\pi}{h} \quad (2.33)$$

where  $X'_{11}=1,8412$ ,  $X'_{21}=3,05$ ,  $X'_{01}=3,83$ ,  $X'_{31}=4,2$

We can calculate the fields inside the cavity by using Maxwell's equations.

Resonant frequency of the cavity can be found by the equation

$$f_{r(mno)} = \frac{1}{2\pi\sqrt{\mu\epsilon}} \left( \frac{X'_{mn}}{a_e} \right) \quad (2.34)$$

where  $a_e$  is the effective area of the antenna which is caused by the fringing effects and can be given by (Balanis 1996) ;

$$a_e = a \sqrt{\left\{ 1 + \frac{2t}{\pi a \epsilon_r} \left[ \ln \left( \frac{\pi a}{2t} \right) + 1.7726 \right] \right\}} \quad (2.35)$$

### 2.1.3 Feeding Methods of MSA

Basic feeding techniques for MSA are coaxial feeding and microstrip line feeding.

Both of them are contacting type feeding as shown in Figure 2-9.

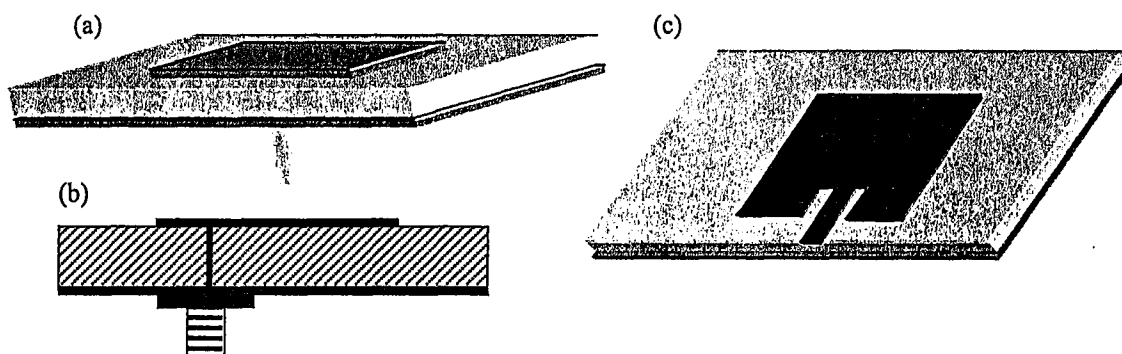


Figure 2-9 Feeding techniques of MSA (a),(b) coaxial feeding (c) microstrip feeding

These techniques are very similar in operation and offer freedom of choice to select antenna input impedance. Since input impedance of the MSA changes while traveling on the patch.

These feeds excite the patch through the coupling of the  $J_z$  feed current to the  $E_z$  field of the dominant patch mode;

$$\text{coupling} \rightarrow \int_v E_z J_z dv \approx \cos \frac{\pi s}{L} \quad (2.36)$$

Here  $L$  is the resonant length of the patch and  $s$  is the offset of the feed point from the patch edge

According to the above formula maximum coupling occurs at a radiating edge of a patch

These techniques have the advantage of simplicity but also have many disadvantages; For microstrip feeding technique dielectric constant of the substrate is a disadvantage because if we use a low dielectric constant material for good antenna efficiency then feed line radiates and destroys our antennas radiation. Thus selection of the material is a problem. When using coaxial probes for feeding no problem will occur for a single antenna but when we start using arrays with numerous antennas then all that wiring will become a junk and system will be less reliable because of increasing solder points. Another disadvantage of direct contact feeds is that they do not only excite dominant modes but also excite some higher order modes which causes cross polarization of antennas.

Alternative feeding techniques have developed because of these disadvantages of contacting feeds. Two non conducting techniques widely used are proximity coupled feeding and aperture coupled feeding. These techniques are illustrated in Figures 2-10 and 2-11 (Pozar 1996).

The proximity uses a two layer substrate with microstrip line on the lower substrate terminating in an open stub below the patch which is printed on the upper substrate.

This technique allows the patch to exist on thicker substrate for improved bandwidth. Fabrication is more complex when compared with standard feeds. But it has freedom of choice to adjust the width and length of the feed line which can be

used to match the antenna impedance. Feed line ends just at the center of the antenna but can be adjusted for other applications.

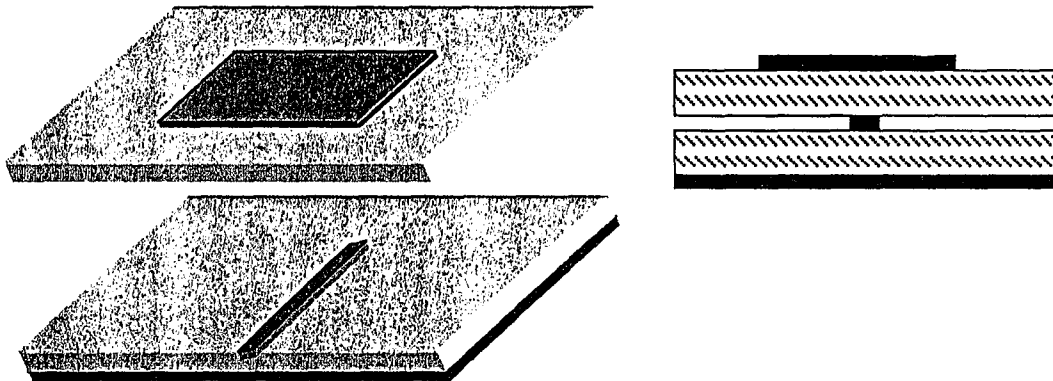


**Figure 2-10 Proximity Coupled Feeding Technique**

### 2.1.3.1 Aperture Coupled Feeding of MSA

Aperture coupled feeding configuration of a MSA uses two parallel substrates separated by a ground plane as seen in Figure 2-8. They use same metallic plate as ground like in proximity coupling but they are not on the opposite sides this time.

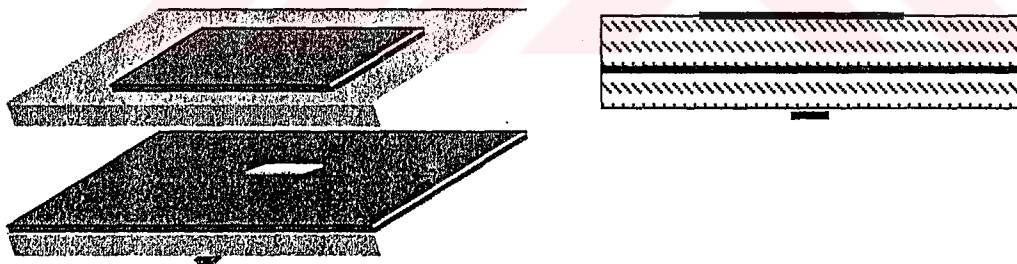


**Figure 2-11 Aperture coupled feeding technique**

There is a small gap on the ground plane called aperture on the separating ground plane. This small aperture couples the electromagnetic field on the microstrip transmission line to the antenna. Coupling aperture is generally smaller than the resonant size so the backlobe radiated by the slot is typically 15-20 dB below the forward main beam. Rectangular shaped apertures are preferred generally because of their increased magnetic polarizability.

We can arrange both layers independently and thus can optimize antenna layer for radiation and microstrip layer for transmission by using substrates with adequate dielectric constants. The ground plane also eliminates spurious radiation from the feed from interfering with the antennas radiation pattern. Using this technique gives us the chance to adjust four parameters in order to tune the antenna for optimum performance. These are slot size and position, feed substrate parameters and feed line width (Pozar 1996).

*slot length:* The coupling level is primarily determined by the length of the coupling slot, as well as the back radiation level. The slot should therefore be made no larger than is required for impedance matching.

*slot width:* The width of the slot also affects the coupling level, but to a much less degree than the slot length. The ratio of slot length to width is typically 1/10.

*feed line width:* Besides controlling the characteristic impedance of the feed line, the width of the feed line affects the coupling to the slot. To a certain degree, thinner feed lines couple more strongly to the slot.

*feed line position relative to slot:* For maximum coupling, the feed line should be positioned at right angles to the center of the slot. Skewing the feed line from the slot will reduce the coupling, as will positioning the feed line towards the edge of the slot.

*position of the patch relative to the slot:* For maximum coupling, the patch should be centered over the slot. Moving the patch relative to the slot in the H-plane direction has little effect, while moving the patch relative to the slot in the E-plane (resonant) direction will decrease the coupling level.

*length of tuning stub:* The tuning stub is used to tune the excess reactance of the slot coupled antenna. The stub is typically slightly less than  $\lambda_g/4$  in length; shortening the stub will move the impedance locus in the capacitive direction on the Smith chart.

A very important advantage of the aperture coupled MSA is the increased bandwidth when compared with other feeding techniques. Which have bandwidths of are typically limited to bandwidths of 2%-5%, aperture coupled elements have been demonstrated with bandwidths up to 10 - 15% with a single layer and up to 30-50% with a stacked patch configuration This improvement in bandwidth is primarily a

result of the additional degrees of freedom offered by the stub length and coupling aperture size. The tuning stub length can be adjusted to offset the inductive shift in impedance that generally occurs when thick antenna substrates are used, and the slot can be brought close to resonance to achieve a double tuning effect. Use of a stacked patch configuration also introduces a double tuning effect (Pozar 1996).

We need much space in our application since lot of circuitry will be placed on the substrate for phase shifters. Another advantage of aperture coupled feeding is that since its feed layer and antenna layer is separated nearly completely there is so much free space on the feed layer for active or passive circuit elements. So this makes them more suitable than other type of feeding especially for phased array antennas.

### 2.1.3.2 Applying Cavity Model to Aperture Coupled MSA

Above we modeled a MSA by cavity modeling method with a coaxial or a microstrip line feed. There electric field was induced by contacting feeds. Here we model a non contacting feed by placing boundary conditions for E and H fields as seen on Figure 2-12. We can model an aperture fed by a microstrip line as a magnetic current source  $M$  determined by the equation  $M=2E^a \wedge z$  where  $E^a$  is the aperture electric field.

$$E^a = \frac{V_0 \sin k^a (L^a / 2 - |y - y_0|)}{W^a \sin(k^a L^a / 2)} \quad (2.37)$$

$$x_0 - w^a / 2 \leq x \leq x_0 + w^a / 2$$

$$y_0 - L^a / 2 \leq y \leq y_0 + L^a / 2$$

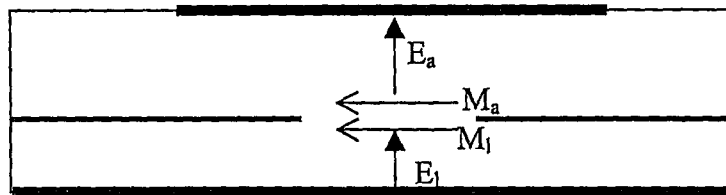


Figure 2-12 Boundary conditions at an aperture fed by a microstrip line

If we assume that magnetic current source is uniformly distributed in the volume above the slot. Equivalent electric current density can be written as;

$$J_m = \frac{2V_0 \sin k^a (L^a / 2 - |y - y_0|)}{tW^a \sin(k^a L^a / 2)} y \quad (2.38)$$

From Maxwell's equations we can obtain electric and magnetic fields inside the cavity with perfect magnetic walls. For dominant  $TM_{10}$  mode electric and magnetic fields are given as;

$$E^i = A \cos\left(\frac{\pi x}{a}\right)z \quad (2.39)$$

$$H^i = B \sin\left(\frac{\pi x}{a}\right)y \quad (2.40)$$

Where A and B are constants evaluated from aperture coupling point, substrate thickness and permittivity.

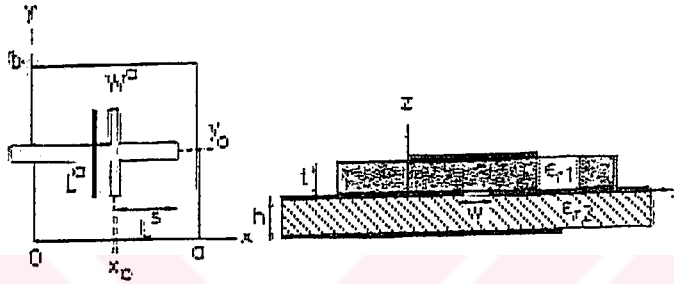


Figure 2-13 Aperture coupling configuration

The radiating magnetic current source at the edges of the cavity is  $K(x, y) = tE^i(x, y) \wedge I$  at the edges of the cavity which is caused by the fringing fields. Radiated power can be calculated and resultant efficiency is

$$\delta_{eff} = \frac{1}{Q} = \frac{P_{rad} + P_{cu} + P_d}{2\omega W_{elec}} \quad (2.41)$$

The admittance of the antenna at the aperture is given by;

$$Y_{ant} = [P_{rad} + P_{cu} + P_{di} + 2j\omega(W_{elec} - W_{mag})] |V_0|^2 \quad (2.42)$$

Due to the stored energy in aperture we have also a susceptance component given by;

$$Y_{ap} = -\frac{2j}{Z_{ca}} \cot\left(k^a \frac{L_a}{2}\right) \quad (2.43)$$

$$Y_{tot} = Y_{ap} + Y_{ant} \quad (2.44)$$

This is the admittance at the coupling aperture. It can be observed on the transmission line by a transformer effect as can be seen in Figure 2-10. We should obtain the transformer ratio in order to calculate the impedance seen on microstrip line. We can evaluate this by rating voltages on transmission line and the aperture to each other. This ratio can be given by the formula;

$$\Delta V = \int_{slot} E^a \wedge h^i ds \quad (2.45)$$

Then  $Y_1$  can be calculated as;

$$Y_1 = \frac{Y_{tot}}{\Delta V^2} \quad (2.46)$$

and if we add the stub impedance starting from the aperture;

$$Z_{in} = Z_1 - jZ_c \cot(k^l L_s) \quad (2.47)$$

Radiation characteristics of an aperture coupled MSA do not differ very much from a contact fed MSA very much (Himdi et al. 1990).

## 2-2 Phased Array Theory

### 2-2-1 Antenna Arrays

Antenna array is a group of similar antennas arranged in various configurations to shape radiation pattern with proper amplitude and phase relations. Shaping the beam gives us flexibility in our applications.

The electromagnetic field of an array is the vector superposition of the fields produced by each similar antenna element in the array. While determining the radiation pattern of an antenna array we first calculate the array factor and then multiply it by array factor. This process is called the pattern multiplication.

Array factor is a function of the number of elements, their relative magnitude and relative phases, geometrical arrangement and their spacing.

In case of uniform linear arrays identical antennas are spaced uniformly spaced along a straight line and fed with currents with equal magnitude and phase. In this case array factor is

$$AF(\psi) = \frac{1}{N} \left| \frac{\sin(N\psi/2)}{\sin(\psi/2)} \right| \quad (2.48)$$

where  $\psi = kd \cos \phi + \beta$

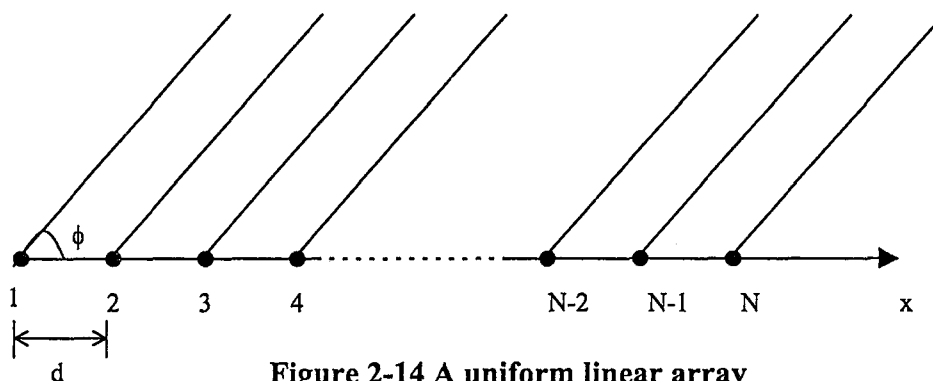


Figure 2-14 A uniform linear array



Here  $N$  is the number of antennas in the array  $d$  is the distance between antennas,  $\beta$  is the phase difference between antennas  $\phi$  is the observation point of the radiation. This illustration can be seen on Figure 2-14.

By the above formula we can calculate the array factor of the antenna array. An antenna arrays radiation pattern is determined by the pattern multiplication method. We calculate the total array antenna pattern is got by multiplying the array pattern by the element pattern

As number of antennas in the array increases the main lobe narrows and more side lobes occur.  $N-2$  side lobes and 1 main lobe occur for each period of AF ( $\psi$ ). Side lobes peaks decreases with increasing  $N$  also.

### 2.2.2 Planar Arrays

If we place radiators along a rectangular grid we form a planar array as can be seen in Figure 2-15. By using planar array additional variables can be controlled for an antenna array. Planar arrays provide more symmetrical patterns with lower side lobes. They can be used to scan the main beam of the antenna toward any point in space. Array factor for a planar array with  $M$  radiators on  $x$  axis and  $N$  radiators on  $y$  axis is given by the formula;

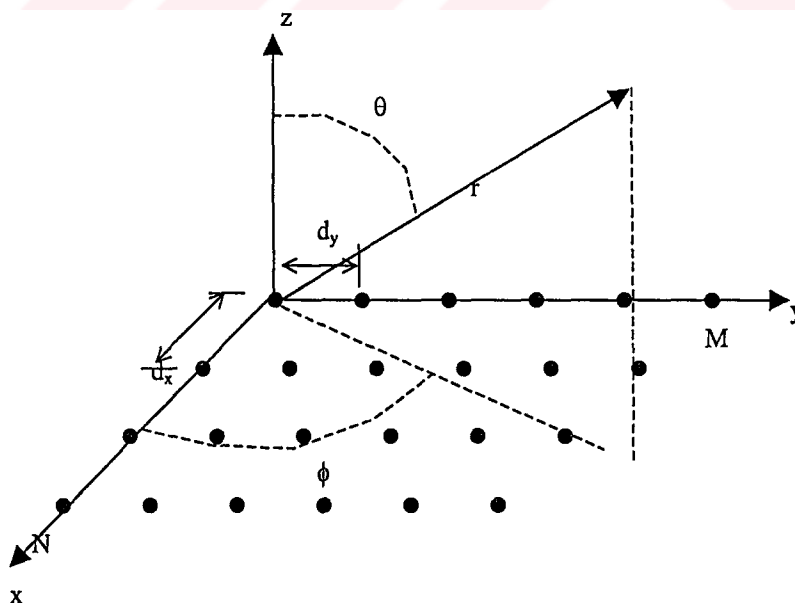


Figure 2-15 Planar array

$$AF_n(\theta, \phi) = \left\{ \frac{1 - \sin\left(\frac{M\psi_x}{2}\right)}{M \sin\left(\frac{\psi_x}{2}\right)} \right\} \left\{ \frac{1 - \sin\left(\frac{N\psi_y}{2}\right)}{N \sin\left(\frac{\psi_y}{2}\right)} \right\} \quad (2.49)$$

where

$$\begin{aligned} \psi_x &= kd_x \sin \theta \cos \phi + \beta_x \\ \psi_y &= kd_y \sin \theta \sin \phi + \beta_y \end{aligned} \quad (2.50)$$

When the spacing between the elements is equal to or greater than  $\lambda$  multiple maxima are formed which are called grating lobes. In order to avoid grating lobes spacing must be kept smaller than  $\lambda$ .

Here relative phases between antennas both in x and y directions are independent of each other and can be used to direct the beam to any point in space. But multi beams can occur because of this so it is generally preferred to adjust them relative to each other (Lo 1987).

### 2.2.3 Circular Arrays

A different form of an array is the circular array. It can be analyzed as a linear or a planar array. Elements are placed on a circular ring. It is very suitable for phased array applications because of narrow main beam and easy beam steering to any point. Mathematical calculations for such array is a little bit complex and time consuming but the array factor when all currents are equal can be given by the following formula;

$$AF(\theta, \phi) = NI_0 \sum_{m=-\infty}^{+\infty} J_{mN}(k\rho_0) e^{jmN(\pi/2 - \beta)} \quad (2.51)$$

Where  $J_p(x)$  is the Bessel function of the first kind and zero order Bessel function  $J_0(k\rho_0)$  is called the principal term. For a circular array with large number of elements, the term  $J_0(k\rho_0)$  alone can be used.

For very large number of antennas directivity becomes the number of antennas N (Balanis 1996).

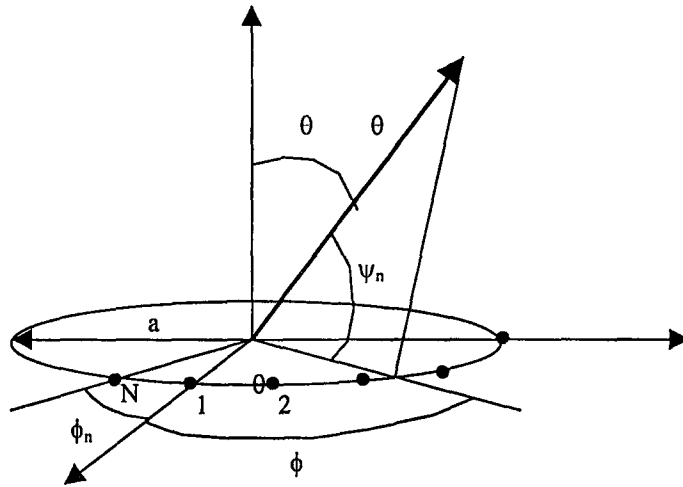


Figure 2-16 Circular array configuration

#### 2-2-4 Phased Array Theory

As stated above relative phase difference between antennas is a way to control the main beam of the antenna. Thus we call an array antenna, whose main beam direction or radiation pattern is controlled by phase difference between array elements, a phased array antenna.

For a linear array the array factor is given by (2.48). Here array factor is maximum when  $\psi=0$ ;

$$\psi = kd \cos \theta_0 + \beta \quad (2.52)$$

$$\beta = kd \cos \theta_0 \quad (2.53)$$

where  $\theta_0$  is the angle of the main beam direction. Using (2.53) once main beam angle is defined relative phase difference can be evaluated.

If we find the relative phase difference as  $\alpha$  in Figure 2-17 then phase values of the antenna currents are;

$$\beta_1 = 0, \beta_2 = \alpha, \beta_3 = 2\alpha \dots$$

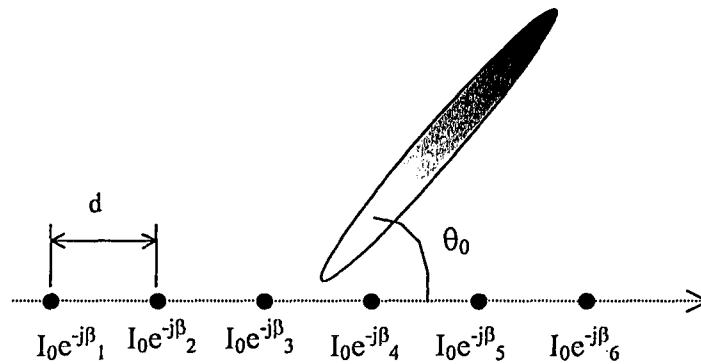


Figure 2-17 Linear phased array antenna feed currents

Some demonstrations of effects of phase shift on array factor for a 2 antenna array can be seen on Figure 2-18.

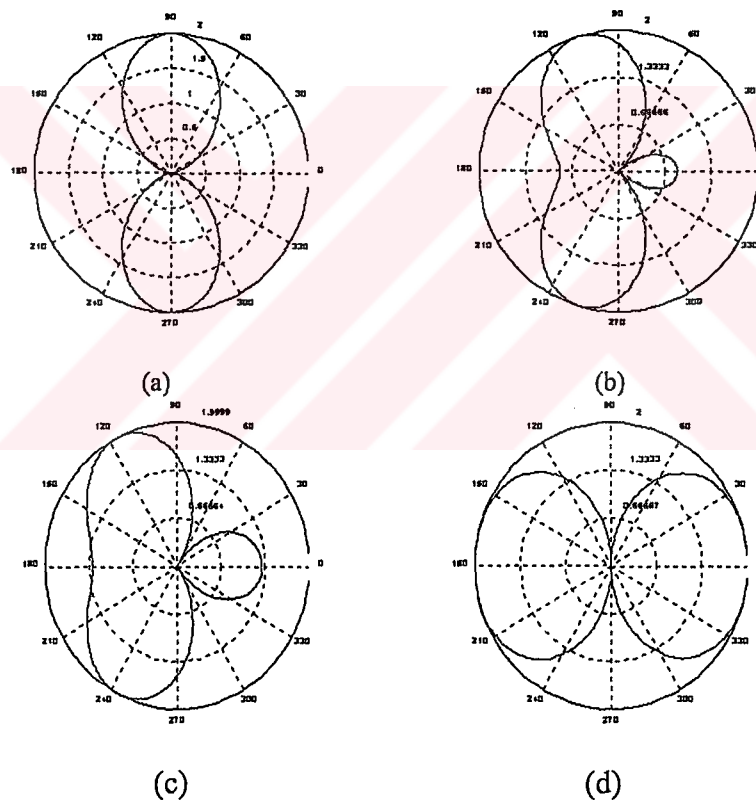


Figure 2-18 Phase shifts of (a)  $0^\circ$  (b)  $45^\circ$  (c)  $90^\circ$  (d)  $180^\circ$  applied to a 2 antenna array

For a planar array the computations do not differ very much. Array factor for a planar array is given by 2.49. here AF gets its maximum value where  $\psi_x$  and  $\psi_y$  are equal to zero as in the case for a linear array.

$$\begin{aligned}\psi_x &= kd_x \sin \theta_x \cos \phi_x + \beta_x = 0 \\ \psi_y &= kd_y \sin \theta_y \sin \phi_y + \beta_y = 0\end{aligned}\quad (2.54)$$

thus maximum point is dependent on phase difference value  $\beta_x$  and  $\beta_y$ .

$$\begin{aligned}\beta_x &= -kd_x \sin \theta_x \cos \phi_x \\ \beta_y &= -kd_y \sin \theta_y \sin \phi_y\end{aligned}\quad (2.55)$$

Here we can see that one can decide the phase difference between antennas in both directions x and y if the direction of point in space is known. Phases  $\beta_x$  and  $\beta_y$  can be adjusted independent of each other so that main beam formed by the x direction phase shift is different from the y direction formed main beam. But practically this not the case to be preferred since radiation pattern will be deformed very much. So we adjust phase shifts in both directions in order to have a main beam (Lo 1987);

$$\begin{aligned}\theta_x &= \theta_y = \theta_0 \\ \phi_x &= \phi_y = \phi_0\end{aligned}\quad (2.56)$$

thus solving both equations we evaluate;

$$\tan \phi_0 = \frac{\beta_y d_x}{\beta_x d_y}\quad (2.57)$$

$$\sin^2 \theta_0 = \left( \frac{\beta_x}{kd_x} \right)^2 + \left( \frac{\beta_y}{kd_y} \right)^2\quad (2.58)$$

For a circular array one can direct the beam with adjusting phase difference between elements. Array factor for circular array is given by

$$AF(\theta, \phi) = \sum_{n=1}^N I_n e^{j[k a \sin \theta \cos(\phi - \phi_n) + \beta_n]}\quad (2.59)$$

where  $\beta$  denotes relative phase between antennas. To direct the main beam in the  $(\theta_0, \phi_0)$  direction phase excitation of the  $n^{\text{th}}$  element can be given as (Balanis 1996);

$$\beta_n = -ka \sin \theta_0 \cos(\phi_0 - \phi_n)\quad (2.60)$$

General scheme for a phased array antenna is shown in Figure 2-19.

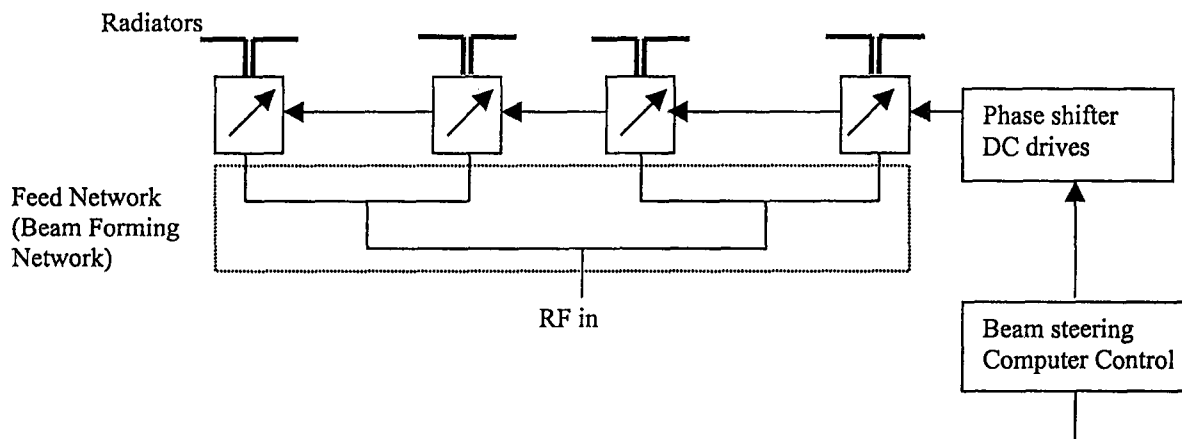


**Figure 2-19 Scheme of a phased array antenna**

As illustrated in Figure 2-19 a phased array antenna consists of an array of radiating elements with each radiating element connected to a phase shifter. The phase shifter controls the phase of the radiated signals at each radiating element in order to locate the beam into desired angle. A feed network (in other words beam forming network) is used to distribute the output signal from the RF in to radiating elements and provide the required aperture distribution for beam shape and side lobe control. Phase shifters are controlled by a computer which controls the DC drives of the phase shifters.

In Table 2-2 properties effected by different layers of a phased array are shown. Dark parts of the table indicates that corresponding property is effected by the layer of that column.

Choosing the appropriate part for each layer is an important phenomenon for a phased array and this selection changes from one application to another.

The radiator must be selected on the basis of meeting all the antenna performance , physical packaging and environmental requirements at minimum cost (Tang 1987).

**Table 2-2 Properties effected by layers of a phased array antenna**

	Feed Network	Radiator	Phase shifter
Number of simultaneous beams	Shaded		
Monopulse sum and difference beams	Shaded		
Peak and average side lobe level	Shaded	Shaded	Shaded
Polarization	Shaded		
Spatial Scan coverage	Shaded		
Beam Switching speed			Shaded
Tunable and instantaneous bandwidth	Shaded	Shaded	Shaded
Peak and average power	Shaded	Shaded	Shaded
Thermal and overpressure loads	Shaded	Shaded	
Operating temperature range			Shaded
Prime power			Shaded
Size weight and cost	Shaded	Shaded	Shaded
Producibility maintainability and reliability	Shaded	Shaded	Shaded

### 2-3 Phase Shifter Design for Antenna Arrays

Phase shifter is one of the most important criteria when designing a phased array antenna. A selection of digital versus analog phase shifter comes in to consideration in design procedure.

Digital phase shifters are easy to design and implement. One basic logic of a digital phase shifter is to design transmission lines of different length and switch between them for different phases. This is illustrated in Figure 2-20. Performance advantages of such a phase shifter is that; it is linear, reliable and it has low insertion loss.

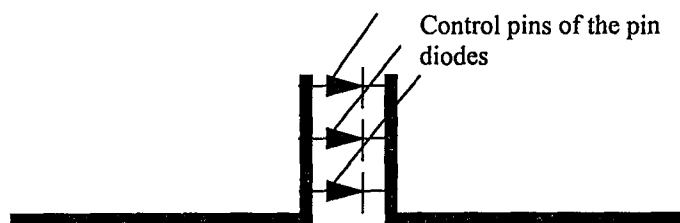
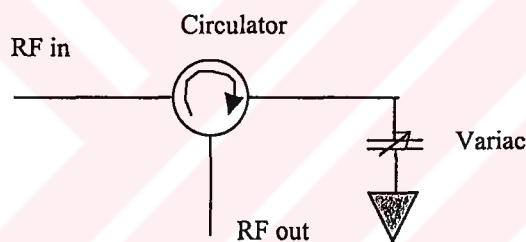


Figure 2-20 3 phase level digital phase shifter

Major disadvantage of such a phase shifter is that it occupies too much space if one wants to shift the phase angle to more than two values. This is an important parameter because especially for low dielectric substrates wavelength is not so small inside the dielectric media and thus space under consideration is worth to concern.

This situation does not differ very much in other digital phase shifters because one must add new components always for each phase to be adjusted. This makes circuit more complex and since coupling occurs with too close objects design also gets more complex for such applications.

A continuous phase shift can be obtained from an analog phase shifter. In most simple case a varicap terminating a circulator as can be seen in Figure 2-21 a high reflection coefficient and phase of the reflected wave will vary continuously (Garver 1976).



**Figure 2-21 Analog phase shifter with a circulator**

The variable capacitance of varicaps is a nonlinear function of bias voltage and the RF. This non linearity requires the drive voltage to be distorted to give a linear relationship between control voltage and the phase. The capacitance of a varactor changes most rapidly around zero bias so most of the phase shift occurs at that region of biasing. Also losses due to harmonic generation occurs because of varicap characteristics.

Varicap phase shifters use some tuning inductance's also which make them very frequency sensitive and tuning of these inductance's might be required each time because each varicap's capacitance at same voltage may differ from an other.



But an analog phase shifter has the advantage that it does not occupy so much space and lower number of diodes is required which is a more efficient case for power consumption. Also diodes are reverse biased thus very small power is required for phase shift. This is a very important case for mobile users especially. Thus an analog phase shifter is more suitable for this application.

*Phase shifter Selection for a phased array*

Phase shifter selection for a phased array antenna is considered by;

1. Operating frequency and bandwidth
2. Peak and average RF power
3. Insertion Loss
4. Switching time
5. Size weight and drive power
6. Phase quantization error
7. Analog or digital control

Most important criteria for selecting a phase shifter is the operating frequency and bandwidth and its insertion loss at that frequency. Frequency tunable phase shifters are preferred for application elasticity but increase the cost of the antenna. Another important criteria is the selection of switching type; analog or digital. Digital phase shifters are easy to implement and design but they probably cover more space than an analog phase shifter. However analog phase shifters are less reliable and hard to design but they give more flexibility as to the application.

---

CHAPTER THREE

DESIGN AND IMPLEMENTATION

---

### 3.1 Design Of An Aperture Coupled Circular MSA At 1550 Mhz

Design of an aperture coupled circular MSA involves two stages ; Designing a circular patch for 1550 MHz, designing an aperture coupled feed for the specified frequency.

#### 3.1.1 Design Of A Circular Patch

In order to design a circular patch antenna, we should first define relative permittivity of the substrate ( $\epsilon_r$ ), operating frequency ( $f_r$ ) and thickness of the substrate ( $t$ ).

After determining these parameters we can calculate the radius of the antenna which finishes our design procedure. We calculate the effective radius of the patch first (Balanis 1996);

$$a_e = \frac{1.8412c}{2\pi f_r \sqrt{\epsilon_r}} \quad (3.1)$$

then we can evaluate the real patch radius from the effective area;

$$a = \frac{F}{\sqrt{1 + \frac{2t}{\pi \epsilon_r F} \left[ \ln \left( \frac{\pi F}{2t} \right) + 1.7726 \right]}} \quad (3.2)$$

where

$$F = \frac{8.791 \times 10^9}{f_r \sqrt{\epsilon_r}} \quad (3.3)$$

In our application operating frequency is considered to be 1550 MHz which is a suitable frequency for LMSS applications. Dielectric material selection is the next step in design of the antenna then.

Available substrates for use were two different plexiglas materials one is white and one is transparent and epoxy with one side covered with copper. Dielectric constant for the plexiglas is measured as 2.35 and for the epoxy is 2.4. Thickness of the transparent plexiglas is 5 mm , white plexiglas is 3 mm and epoxy is 1 mm. Thus plexiglas substrates seems a more suitable material for design.

A problem with plexiglas is that it has no metallic coating over it so we need to stick a metal plate for the patch. Since ground layer is mounted on the feed layer for an aperture coupled MSA no problem will occur. I used a sticky aluminum foil on the plexiglas for the patch.

Calculated radius for white plexiglas substrates is 3.3 cm , for transparent substrate is 3.2 cm and for the epoxy is 3.5 cm. All results and characteristics are given in Table 3.1 These three antennas were built up and tested. The testing feed aperture was used as  $L_a = 2.2$  cm  $W_a = 2.5$  mm and width of the transmission line is 2 mm.

**Table 3.1 Available Substrates Properties**

Substrate Material	Dielectric constant	Thickness	Radius of the antenna
White Plexiglas	2.35	3.2 mm	3.3 cm
Transparent Plexiglas	2.35	5 mm	3.2 cm
Epoxy	2.4	1 mm	3.5 cm
GML1000	3.02	1.6 mm	3.2cm

From Figure 3-1 and 3-2 we can measure the directivity and the gain of the antenna in E and H fields. HPBW of the antenna in E field of measurement is 120 degree and from the H field measurement is 100 degree Transmission loss between two identical antennas is  $-17.6$  dB for a distance of 30 cm (measured by spectrum analyzer). Thus by using Friis equation given by 3.4 we can calculate the gain of a single antenna as

$$\frac{P_r}{P_t} = \left( \frac{\lambda}{4\pi R} \right)^2 G_o G_{or} \quad (3.4)$$

Where R is the distance between two antennas and G's are the gains of the antennas. Since we use identical antennas we can take them as equal as G. Total transmission loss can be calculated by;

$$P_{r, \log} = 10 \log \frac{P_r}{P_t} \quad (3.5)$$

Thus gain of a single MSA can be calculated as 5.6 dB.

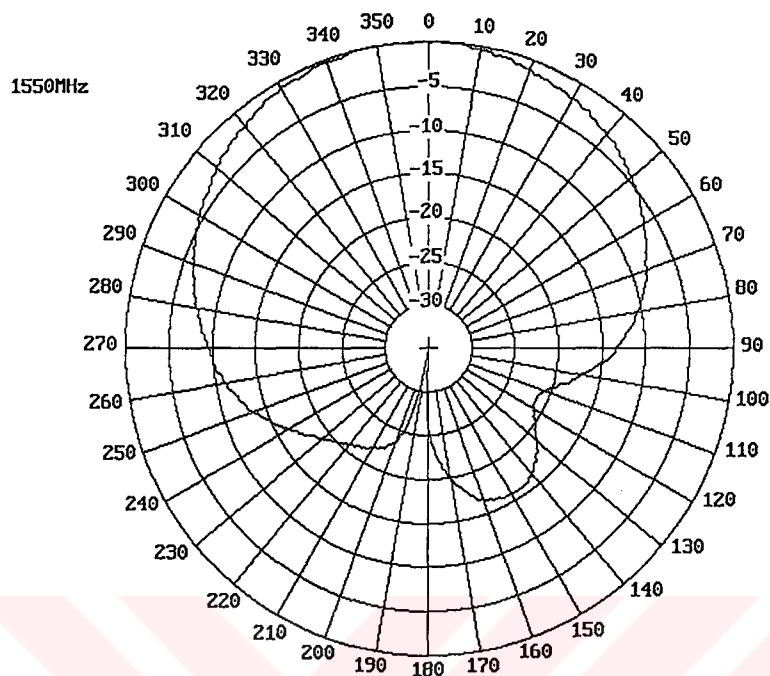


**Figure 3-1 Polar plot of H plane radiation of an aperture coupled circular MSA (dielectric media is GML1000 radius is 3.2 cm)**

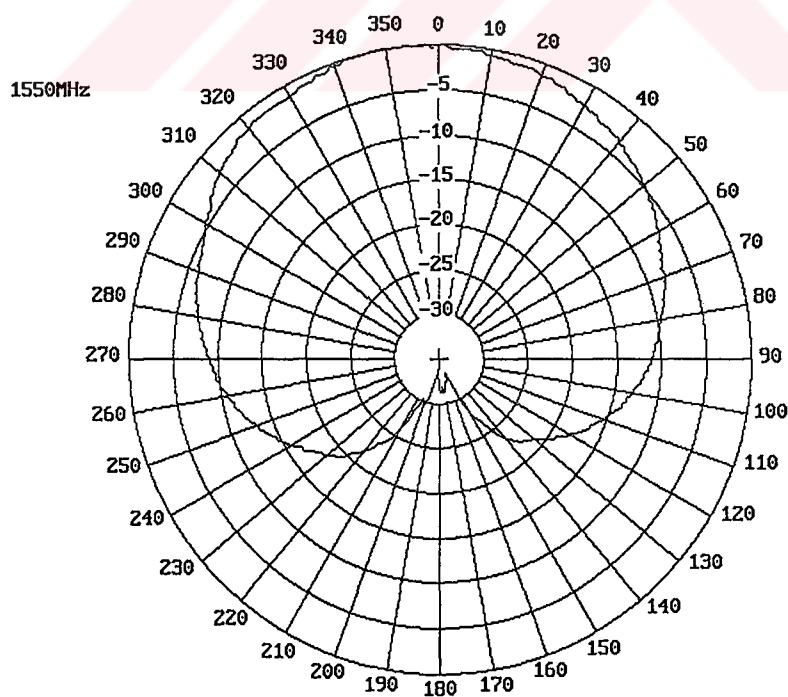


**Figure 3-2 Polar plot of E plane radiation of an aperture coupled circular MSA (dielectric media is epoxy radius is 3.3 cm)**

Power in dB

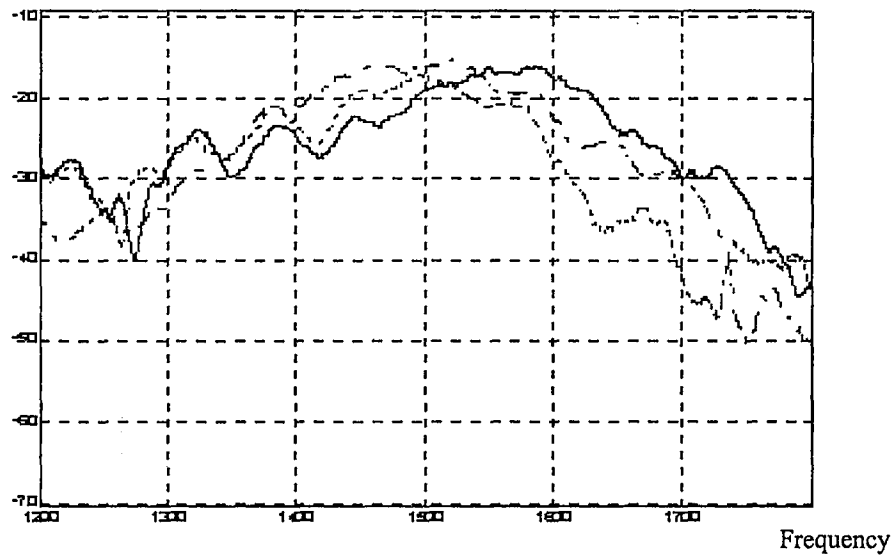


**Figure 3-2 Received power plot of the three antennas. (Continuous line transparent plexiglas, dotted line epoxy, long dotted line is white plexiglas)**

From Figure 3-2 we can analyze that if the antenna substrate is thicker we have a wider bandwidth as was stated in the theory of microstrip antennas. 3 dB bandwidth for the transparent plexiglas which is .5 cm thick is nearly 150 MHz where for the white plexiglas it is near 120 MHz and for the epoxy it is near 80 MHz.

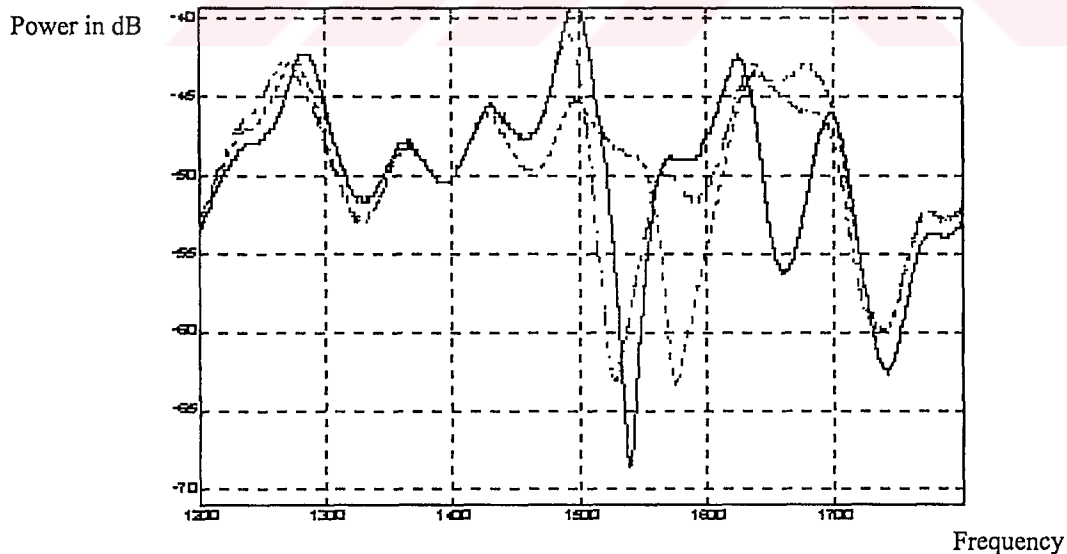


**Figure 3-3 Return Loss analysis of three different materials (continuous line is epoxy, small dotted is white plexiglas and long dotted line is the transparent plexiglas)**

From Figure 3-3 we can observe that epoxy substrate offers us a better match at resonant frequency of the antenna. This means that coupling through the aperture is more strong with thinner and high permittivity substrates. Shift of frequency in white plexiglas substrate might be caused by slight mismatch of relative dielectric constant between two plexiglas materials or because of the thin film coating on the patch metal.

Later on works showed us that GML1000 substrate for antenna layer is a better choice. It showed us a return loss of  $-21$  dB while epoxy did only  $-17$  dB as in Table 3.3. And as can be seen in polar plot diagrams its radiation characteristics are better.

### 3-1-2 Aperture Coupled Feeding

Referring to 2<sup>nd</sup> chapter we can see that aperture coupled feeding consists of a microstrip transmission line coupling to an antenna through a small aperture on its ground plane. Antenna is just placed on the aperture.

Here design procedure covers three main concepts; width and length of the aperture and length of the tuning stub.

Here slot length determines the coupling level from the microstrip line to the antenna. This value is determined mostly by practically except some trivial formulas as given in (Karmakar et al. 1999)  $\lambda_g/10$  value is a suitable value. Here  $\lambda_g$  denotes wavelength in the feed layer dielectric.

Slot width does not effect coupling as the slot length but it should be in good ratio with it. A suggested ratio is  $1/10^{\text{th}}$  of the slot length (Pozar 1996).

Tuning stub is also an important parameter which must be taken into account. The tuning stub is used to tune the excess reactance of the slot coupled antenna. Its length should be near  $\lambda_g/4$  but a little bit smaller. We use this length in order to minimize reactive loading of the transmission line. Shortening the stub will move the impedance locus in the capacitive direction on the Smith chart.

For the feed substrate FR4 was chosen with relative dielectric constant of 5.65 and thickness of 1.5mm . A transmission line was designed with width 2.2mm in order to make characteristic impedance of the line  $50\Omega$ . Aperture is placed 4 cm apart from the feed point .

Wavelength inside a dielectric media can be found by the (2.1). But if we are working with microstrip lines we must use (3.5) because of fringing fields at the edges. (Ludwig 2000)

$$\lambda_g = \frac{\lambda_0}{\sqrt{\epsilon_{eff}}} \quad (3.5)$$

$$\text{and } \epsilon_{eff} = \frac{\epsilon_r + 1}{2} + \frac{\epsilon_r - 1}{2\sqrt{1 + 12\frac{h}{w}}} \quad (3.6)$$

where  $\lambda_0$  is the wavelength in the free space,  $h$  is the thickness of the substrate and  $w$  is the width of the transmission line as can be seen on Figure 3-3.

We calculate the effective permittivity of the material as;

$$\epsilon_{eff}=4.08$$

and wavelength inside the substrate is ;

$$\lambda_g=9.58 \text{ cm}$$

thus tuning stub length ( $L_s$ ) is calculated as

$$L_s \leq 2.39 \text{ cm}$$

and length and width of the aperture is ;

$$L_a=.9 \text{ cm } W_a=1 \text{ mm}$$

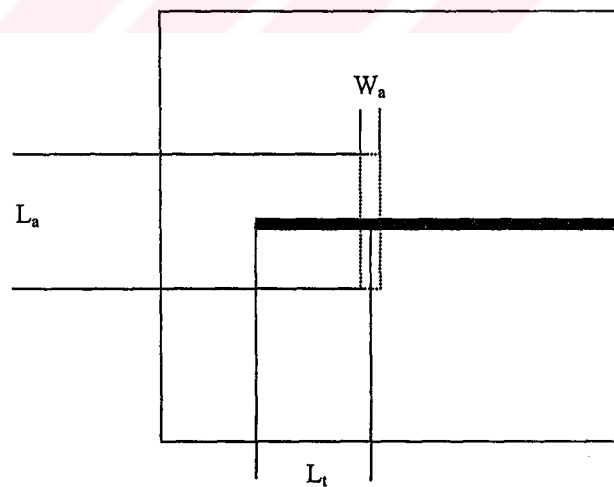


**Figure 3-3 Aperture coupled feeding illustration**

Feed configuration stated above is implemented on a FR4 substrate and tested with the antennas designed in section 3-1.

Return loss measurement was made with the measurement system shown in Figure 3-4

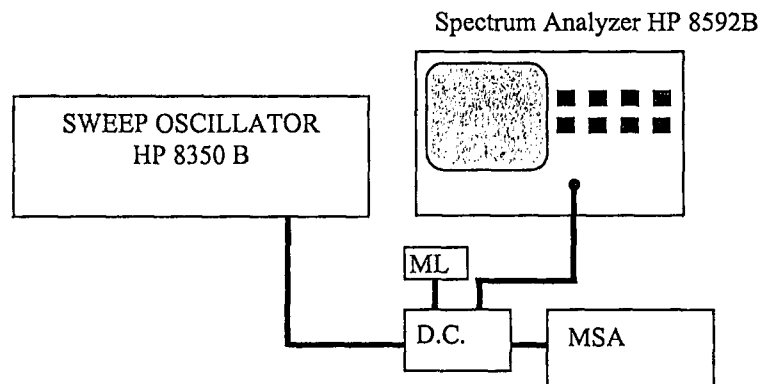


Figure 3-4 Return loss measurement system with Spectrum Analyzer

After connecting the aperture coupled feed to the system and mounting the antenna on to it observed results showed that return loss at operating frequency say 1550 MHz is not that good. As we know from previous chapter that coupling could be increased with widening the length of the aperture. Small cuts of .5 mm were made to the both sides of the aperture in order to obtain better results. Results of this work can be seen in table 3-2.

Table 3-2 Return Loss values of the aperture coupled feed.

$L_a/W_a$ (mm)	Patch on White plexiglas	Patch on Epoxy
.1/.1	.1 dB	.5 dB
1.2/.1	.3 dB	1 dB
1.4/.1	1.3 dB	2 dB
1.6/.15	2 dB	3.5 dB
1.8/.15	4 dB	7 dB
2/.2	5 dB	7.5 dB
2.2/.24	7 dB	11 dB

Data in table 3-2 is obtained with line width of 2.2 mm on substrate with dielectric constant 5.65 and tuning stub length of 2.4 cm.

Increasing aperture length and width will also increase coupling but it will also increase back radiation so it should be kept where the matching of the antenna is achieved. From table 2 we can observe that in order to obtain good coupling to the



patch we should make aperture length near  $\lambda_g/5$  and aperture width  $\lambda_g/50$ . So in this application we can say that MSA is matched at  $L_a = \lambda_g/5$  and  $W_a = \lambda_g/50$

Above results are for the FR4 substrate. A more suitable substrate available for this application is GML1000 from GIL with dielectric constant 3.02. It is a low loss material when compared with the FR4 and is more reliable compared to FR4. More detailed information about this substrate can be achieved at Appendix.

Length of the aperture can be calculated as  $L_a = \lambda_g/5 = 2.6$  cm. for this substrate. Thus we can achieve the width of the aperture as; .26 cm. Thickness of the substrate is 1.6 mm.

Results of the test procedure is shown above.

**Table 3-3 Return loss comparison of aperture size on GML1000**

Aperture $L_a/W_a$	Patch on White P.glas	Patch on Epoxy	Patch on GML1000
20 mm/ 2.5 mm	-7 dB	-10 dB	-12 dB
22 mm /2.5 mm	-9 dB	-14 dB	-17 dB
24 mm/2.5 mm	-10 dB	-17 dB	-21 dB

Back radiation measured at  $L_a = 24$  mm and  $W_a = 2.5$  mm is  $-13$  dB when compared with forward lobe which is a satisfactory result for this application.

### 3-2 Aperture Coupled Microstrip Array Design

Second step in implementing a microstrip phased array antenna is to design an array. Most basic type of array is a dual antenna linear array which is also very suitable starting point.

A microstrip array with distance  $\lambda_0/2$  between the antennas is designed. This array with no phase difference between the antennas would have an array factor as illustrated in Figure 3-5

In order to feed antennas at the same phase with  $d = \lambda_0/2$  a feed network on GML1000 substrate was designed. In order to feed antennas at same phase transmission line lengths should be the same. This was taken into account in design procedure. Antenna feed layer can be seen in Figure 3-6.

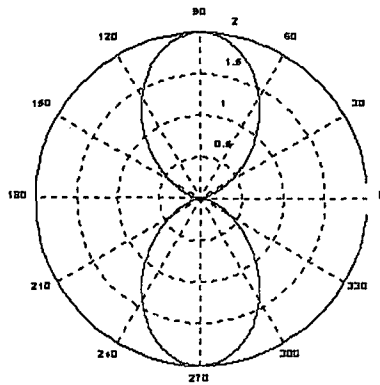


**Figure 3-5 Illustration of a two antenna array with  $d = \lambda_0/2$  and 0 degree phase difference between them.**

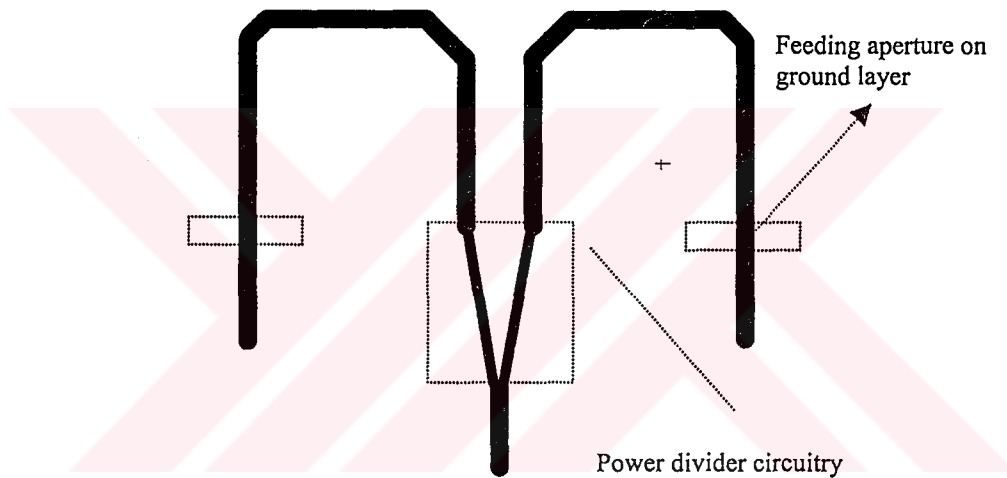


**Figure 3-6 Dual array antenna aperture coupled feed MSA array**

In feed layer illustrated in Figure 3-6 power incident to the network is divided in order to feed dual antennas. This divider is shown in more detailed in Figure 3-7.



**Figure 3-7 Power divider on the feed layer**

Power divider is a Wilkinson equal power divider. In a Wilkinson power divider we use the same as in a typical voltage divider; in order to divide the power into two equal parts equal resistors should be connected to the source. In our case the 50  $\Omega$  feed line at the input. Output impedance does not matter in our case but it should be converted to 100 ohm in order to avoid reflections. This can be done through quarter wavelength transformers. Illustration can be seen in Figure 3-8 (Ludwig et al. 2000)

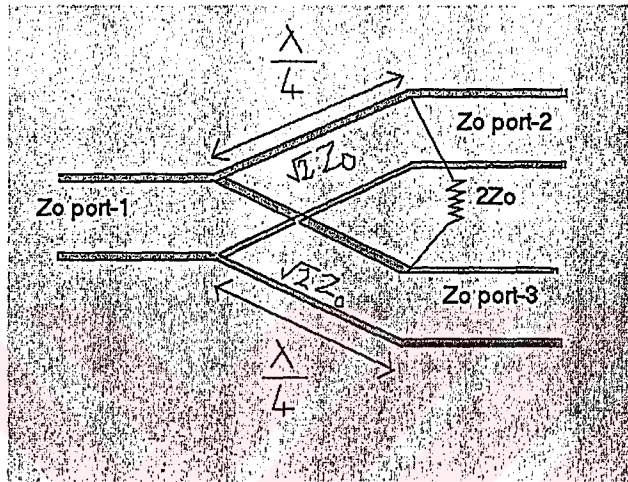


**Figure 3-8 Wilkinson power divider**

In our design output impedance was also taken as 50  $\Omega$  so quarter wavelength parts can be calculated as 71  $\Omega$ . Isolation resistor is to isolate the output ports. If there is a coupling effect between output ports or in other words, the power coming from one output port has an effect on other output port, the perfect division of the power cannot be possible. This isolation resistor avoids the coupling effects of the output ports. Isolation resistor in our application is 100  $\Omega$ .

Width of the transmission line can be calculated via the formula;

$$Z_0 = \frac{Z_{fs}}{\sqrt{\epsilon_{eff} \left( 1.393 + \frac{w}{h} + \frac{2}{3} \ln \left( \frac{w}{h} + 1.444 \right) \right)}} \quad (3.7)$$

$$\text{where } Z_{fs} = \sqrt{\frac{\mu_0}{\epsilon_0}} \text{ as the free space impedance} \quad (3.8)$$

Calculated transmission line widths for 50  $\Omega$  and 70  $\Omega$  lines are respectively; 4 mm and 2.2 mm. (Ludwig et al. 2000)

Performance of the aperture coupled microstrip antenna dual array can be seen in Figures 3-9 and 3-10. Since the feed layer is designed for 1550 MHz return loss and frequency response of the antenna is best at it. Power divider is the most frequency dependent circuit in the feed layer thus it determines the frequency of best match and resonance.

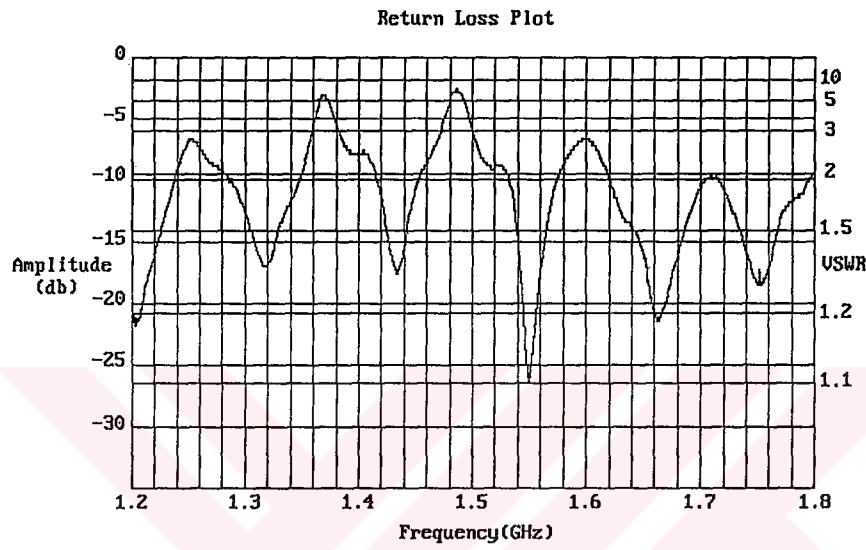


**Figure 3-9 Return loss graphics of dual array**

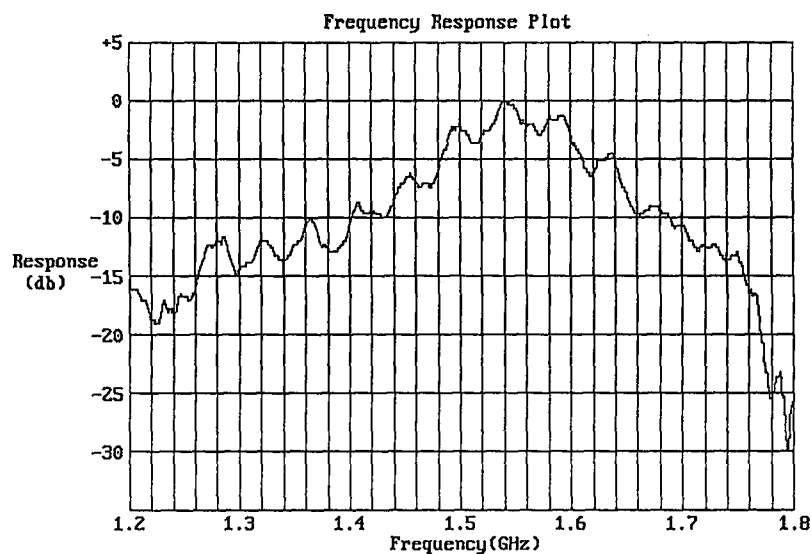


**Figure 3-10 Transmission plot of dual array**

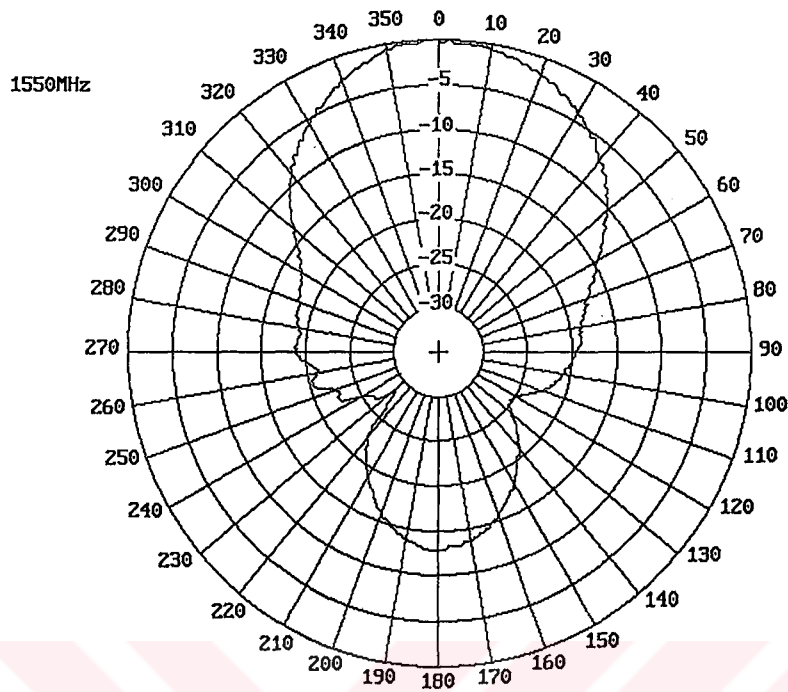


**Figure 3-11 Polar plot of E field radiation pattern of dual array antenna**

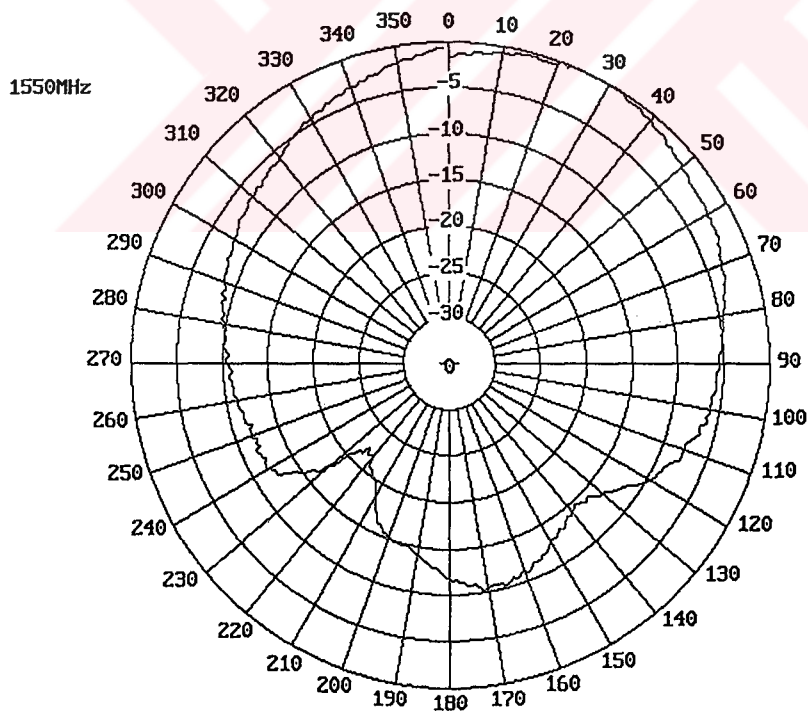


**Figure 3-12 Polar plot of H field radiation pattern of dual array antenna**

Dual antenna array has a narrower beamwidth when compared with a single patch antenna as expected. Even if the backlobe radiation of the array is more when

compared with a single antenna this effect can be explained by the feed layer radiation which occupied much more space.

We can graphically calculate the half power beamwidth (HPBW) as; 50 degrees in E plane and 70 degrees in H plane.

Transmission loss for 30 cm distance using two identical arrays is  $-6,8$  dB by using equations 3.4 and 3.5 we can evaluate the gain and directivity of the array antenna. as 8.57 dB

We can see that a dual array MSA has 3.3 times the normal gain of the antenna. Thus it is more directed to a point in space than a single antenna.

### 3-3 Phase Shifter Design

A very suitable phase shifter for this application is the loaded line phase shifter which is shown in Figure 3-15

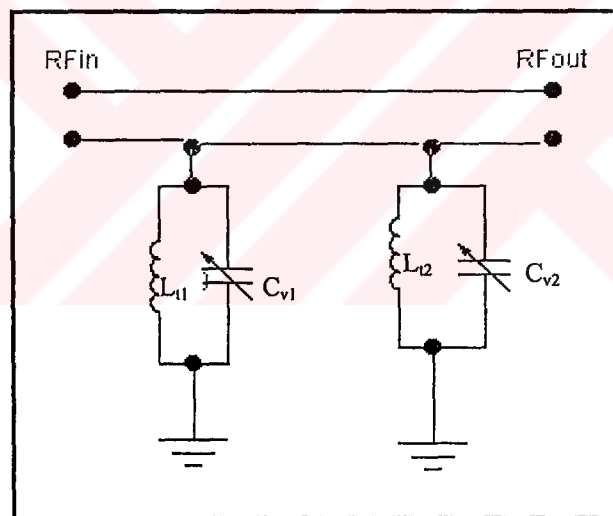
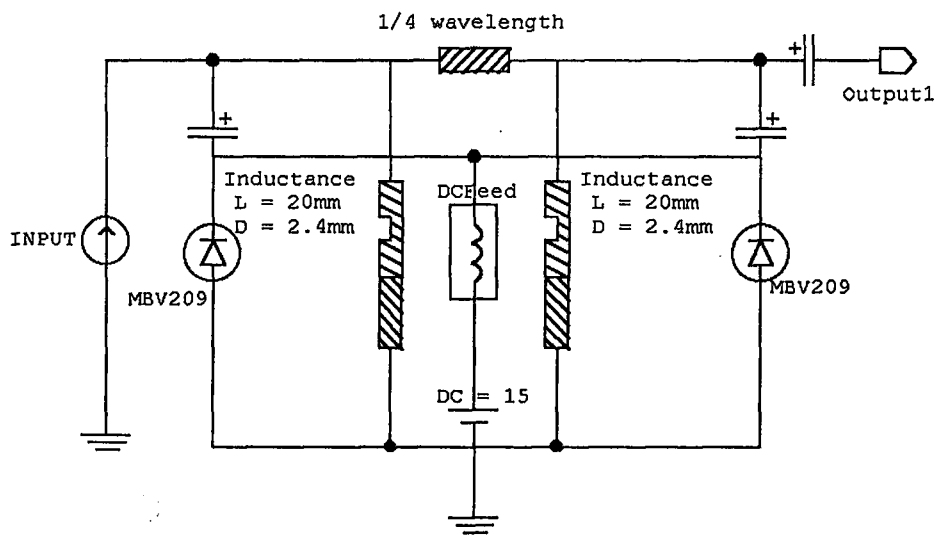


Figure 3-15 Loaded Line Phase Shifter

A continuous loaded line phase shifter consists of two tuning circuits formed by inductance's and variable capacitance's. By tuning capacitance values we tune the reactive load value of the phase shifter which in turn effects the output phase value. (Garver 1976)



**Figure 3-16 Screen capture of simulation using APLAC**

Loaded line phase shifter simulation is performed in APLAC microwave simulation program. This simulation's screen capture can be seen in Figure 3-16

In simulation slit microstrip lines are used instead of coils because they are more suitable for microwave frequencies and also more reliable. A short-circuited microstrip transmission line will act like an inductance or capacitance at different lengths. An impedance graph of a transmission line can be seen in Figure 3-17. As we can observe from the graph a transmission line acts like an inductance for a length of  $0 < l < \lambda/4$ . Since the value of the inductance is a function of the characteristic impedance  $Z_0$  we should increase the characteristic impedance in order to increase the inductance value.

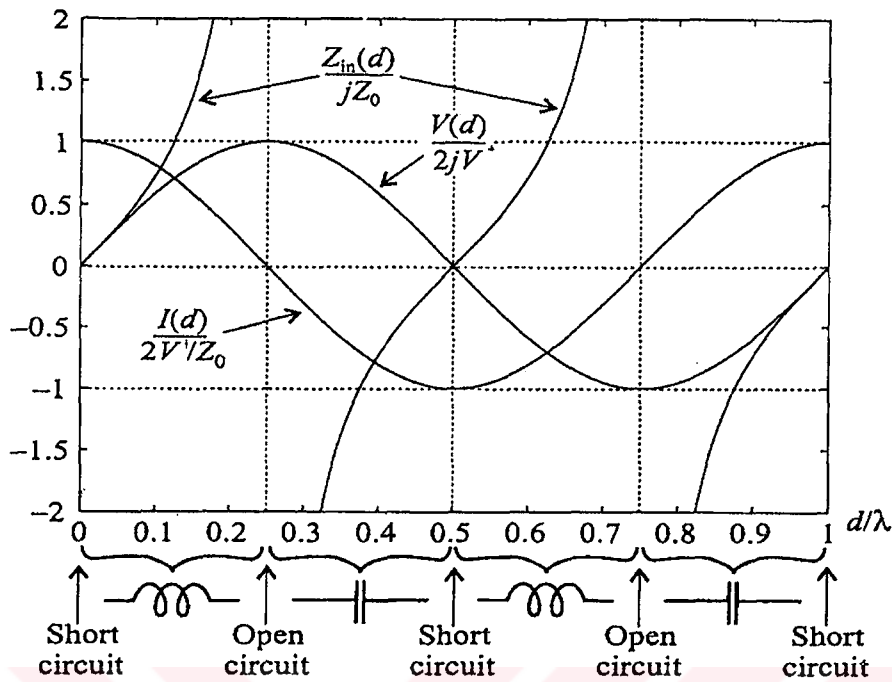


**Figure 3-17 Impedance behavior of an open circuited transmission line**

Characteristic impedance can be increased by decreasing the width of the transmission line. This behavior can be formulated by equation 3.9. This equation is the input impedance formula of a transmission line with characteristic impedance of  $Z_0$  and load of  $Z_L$ . If we make  $Z_L$  equal to 0 then we have equation 3.10 changing input impedance by line length

$$Z_{in} = Z_0 \frac{Z_L + jZ_0 \tanh \gamma l}{Z_0 + Z_L \tanh \gamma l} \quad (3.9)$$

$$Z_{in} = Z_0 \tanh \gamma l \quad (3.10)$$

Simulation results can be seen in Figure 3-18. Here we can see that a zero phase occurs at the peak value of the magnitude plot. We can shift the maximum point by controlling the capacitance value of the varicap. This shift can be observed in Figure 3-19. Here we can see that phase degree at the output versus frequency. At constant frequency we can observe that phase moves to positive direction with increasing voltage.

But an important criteria is to keep the voltage in a region so that insertion loss of the phase shifter is not more than 3 dB. By observing Figure 3-18 we can see that if



the phase shifts out of the region  $-75^{\circ} < \phi < 75^{\circ}$  we will have high insertion losses which can cause unwanted radiation patterns by feeding antennas with unequal currents.

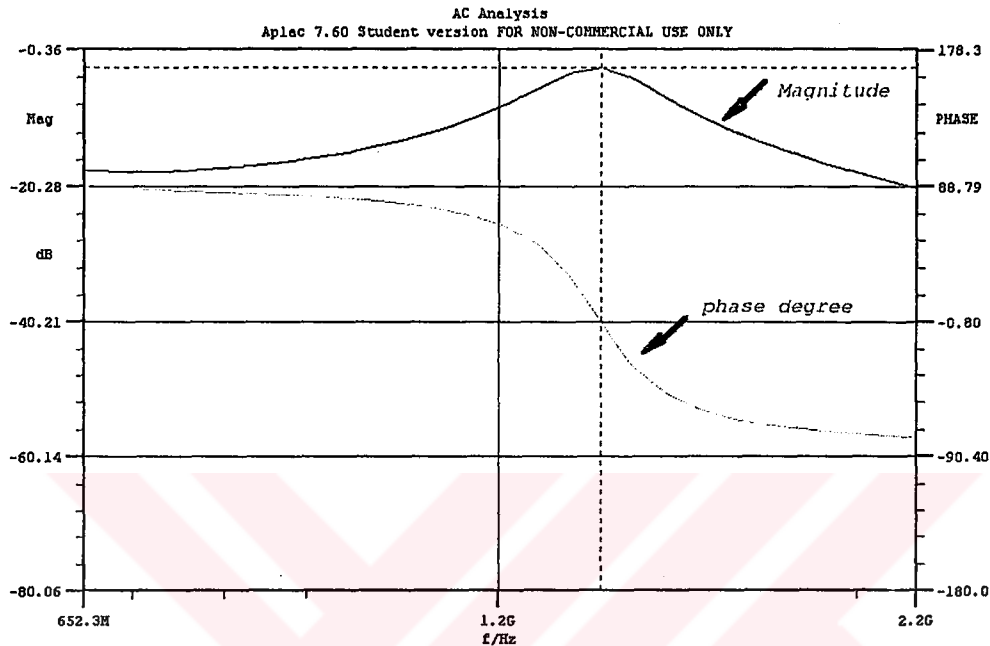


**Figure 3-18 Magnitude and phase response of a Loaded line phase shifter.**

By taking this phenomenon into consideration and observing Figure 3-19 we can decide the bias voltage limitations of the phase shifter. For the simulation case this limitation is described as 15 V to 30V

Tuning is an important criteria which will describe the frequency of operation . Most important tuning element in our simulation circuitry is the inductance which is also the case for the practical circuit.

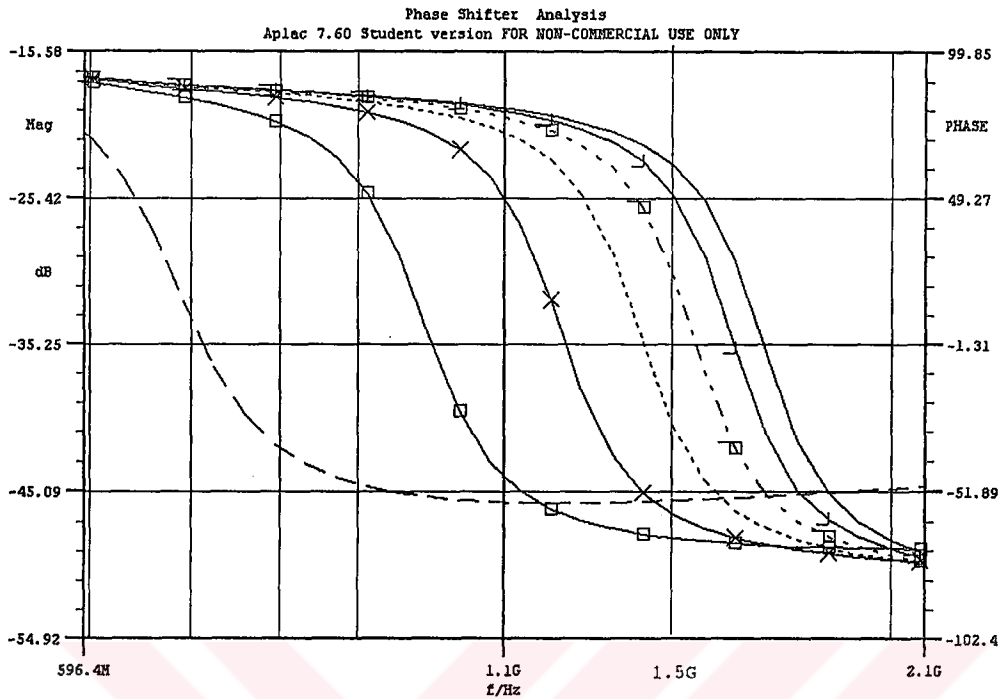


Figure 3-19 Phase Shift of the simulation circuitry at a specified frequency

----- Vb=1V      - - - - - Vb=5V  
 X---X---X Vb=10V      ..... Vb=15 V  
 - - - - - Vb=20 V      - - - - - Vb=25 V  
 ----- Vb=30 V

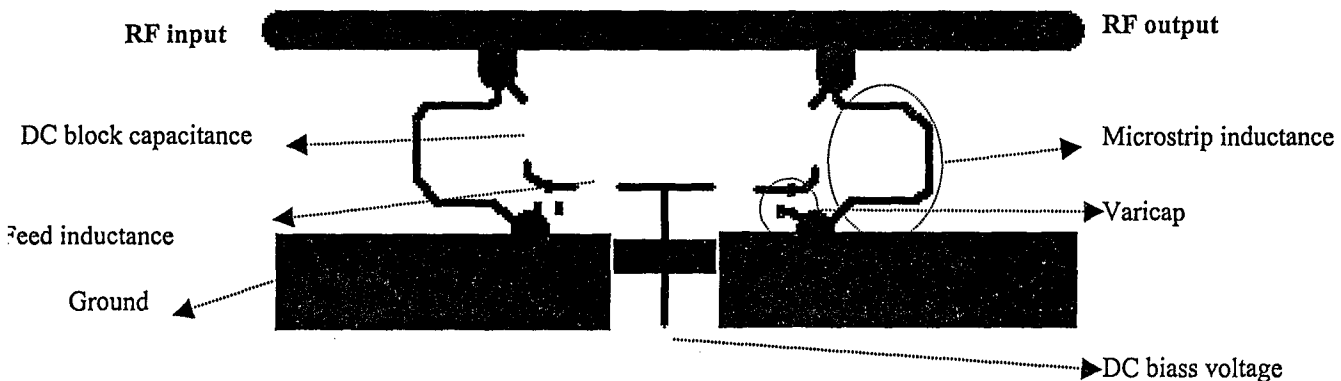


Figure 3-20 Printed circuit diagram of the phase shifter

In circuit illustrated in Figure 3-20 microstrip inductance is of width .8 mm and nearly 2 cm length. Thus calculated impedance for the line is 110 Ω and effective

permittivity is 2.2. Wavelength ( $\lambda$ ) inside the dielectric media can be calculated as 13 cm. So our inductance line is of  $0.16\lambda$  in length. From Figure 3-17 we see that corresponding  $\frac{Z_{in}(d)}{jZ_0}$  ratio is nearly equal to 1;  $Z_{in}$  can be calculated from above equation as  $j110$ . Since our operating frequency is 1500 MHz inductance value is found as 11 nH.

DC feed line in Figure 3.20 is designed to block RF signals in order not to make the DC source act like a load for the RF input. A serial coil inductance is placed on it. The wide part of the line is placed in order to couple the remaining RF signal to the ground placed near by and at the other side of the substrate.

DC voltage must also be separated from the RF part in order not to damage RF devices possibly connected to input and output ports. This is done by capacitors connected in series with the varicap. Since varicap is also a capacitor a value which will not effect its capacitance should be selected. Since our varicap capacitance value is given near 20 pF if we select a blockage capacitance in the range of 1-10 nH it will not be the effective value but will also allow RF signal pass with little loss.

When we apply above conditions to the circuit we can measure a phase control at frequencies near 600 MHz. This is an expected result since varicaps capacitance is a function of both frequency and when the frequency increases capacitance of the varicap decreases to certain values that are nearly short circuit and it can not be controlled efficiently. Thus DC blockage capacitor should be selected near the expected value of the varicap capacitance. Expected value for the varicap capacitance is 1-5 pF so we choose DC blockage capacitance as 1 pF.

Distance between two phase shifting load points is chosen as 3.25 cm which corresponds to  $\lambda_g/4$  value. It is important to choose this value near  $\lambda_g/4$  in order to keep insertion loss small. Results of the test circuitry can be seen in table 3-3.

As we can see from the below table when we increase the bias voltage transmitted power peak value shifts from below of the operating frequency to above. If we observe Figure 3-17 we see that peak value shows us where the phase is zero degrees. And values below peak value have a phase angle higher than zero and above have a phase angle lower than zero.

**Table 3-3 Performance test of the loaded line phase shifter.**

Bias voltage (V)	Insertion loss dB (1500 MHz)	Peak freq (MHz)	Peak transmitted power (dBm)	Estimated Phase (degree)
14.65	3.36	1483	-3.18	-55
15.50	3.25	1486	-3.07	-35
16.50	2.64	1488	-2.85	-20
17.50	2.45	1503	-2.45	0
18.50	2.2	1506	-2.24	5
19.50	2.16	1506	-2.08	12
20.50	2.09	1511	-1.85	18
21.50	2.02	1514	-1.66	24
22.50	2.09	1518	-1.53	30
23.50	2.02	1518	-1.34	36
24.50	2.27	1517	-1.21	42
25.50	2.29	1519	-1.11	48
26.50	2.34	1522	-1	54
27.50	2.34	1523	-.9	60
28.50	2.34	1525	-.85	66
29.50	2.38	1526	-.75	70

Observation of the table 3-3 gives us the following results

- Since maximum point shifts from 1483 to 1526 phase angle gets values from negative to positive. Estimated values from these observations are made by using Figure 3-19
- Insertion loss decreases with increasing voltage thus increasing phase angle. This is due to decreasing capacitance of the varicap thus decreasing energy storage.
- An acceptable insertion loss level is accomplished by this phase shifter in the range of  $-3.36$  dB to  $-2$  dB. This level is also can be considered as constant over the whole phase interval.

### 3-4 Phased Array Antenna Design

In order to design a phased array antenna with using aperture coupled microstrip antennas and an analog phase shifter Phase shifter designed in section 3-3 is implemented on the dual antenna array designed in the section 3-2 for this process.

In order to do this a transmission line 3.25 cm in length is needed for the phase shifter. Since antenna return loss is very low we can assume the antenna as a matched load so distance of the phase shifter to the antenna has negligible effect.

Phase shifting circuitry can also effect coupling through the aperture so we should aware of placing it near. Also metallic structures must be kept in a satisfactory distance to the transmission lines in order not to cause coupling.

Designed feed layer can be seen in Figure 3-21

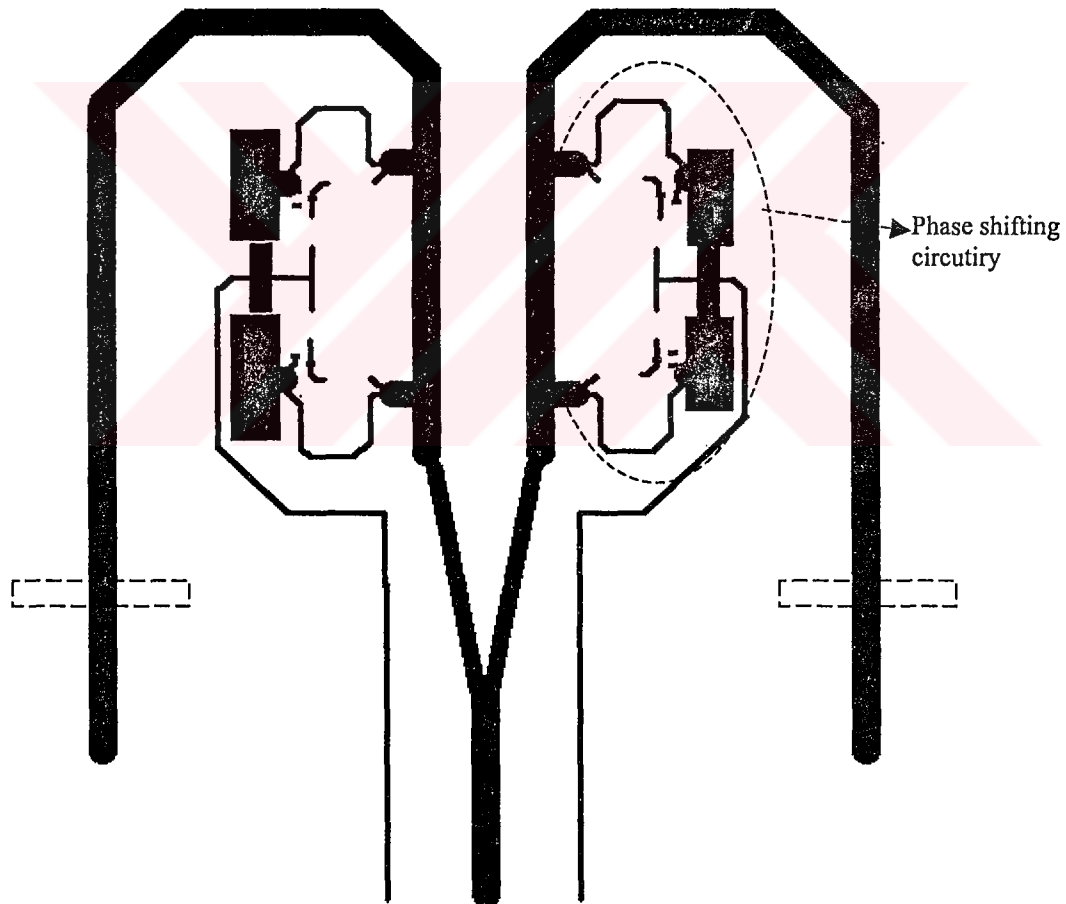


**Figure 3-21 Feed layer with phase shifters  
for aperture coupled dual array MSA**

As a first test of the array return loss tests were made in several voltage levels. Figure 3-22 and 3-23 show graphics of the return losses with changing voltage of different phase shifters respectively.

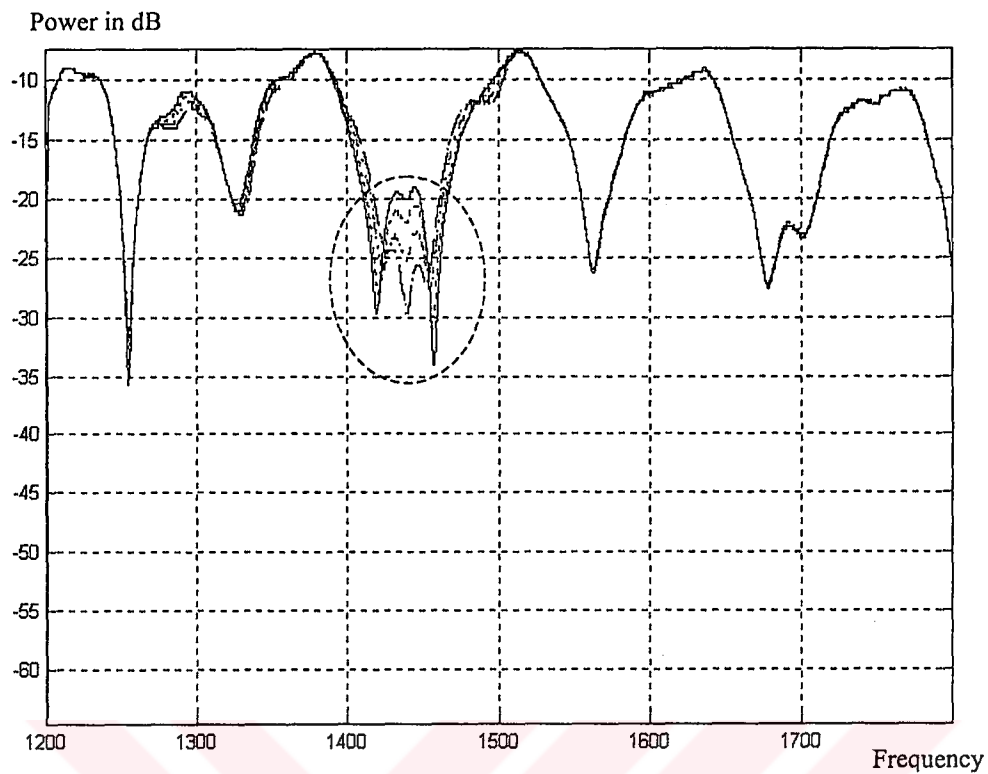


**Figure 3-22 Effect of changing silver colored phase shifter voltage  
on return loss**

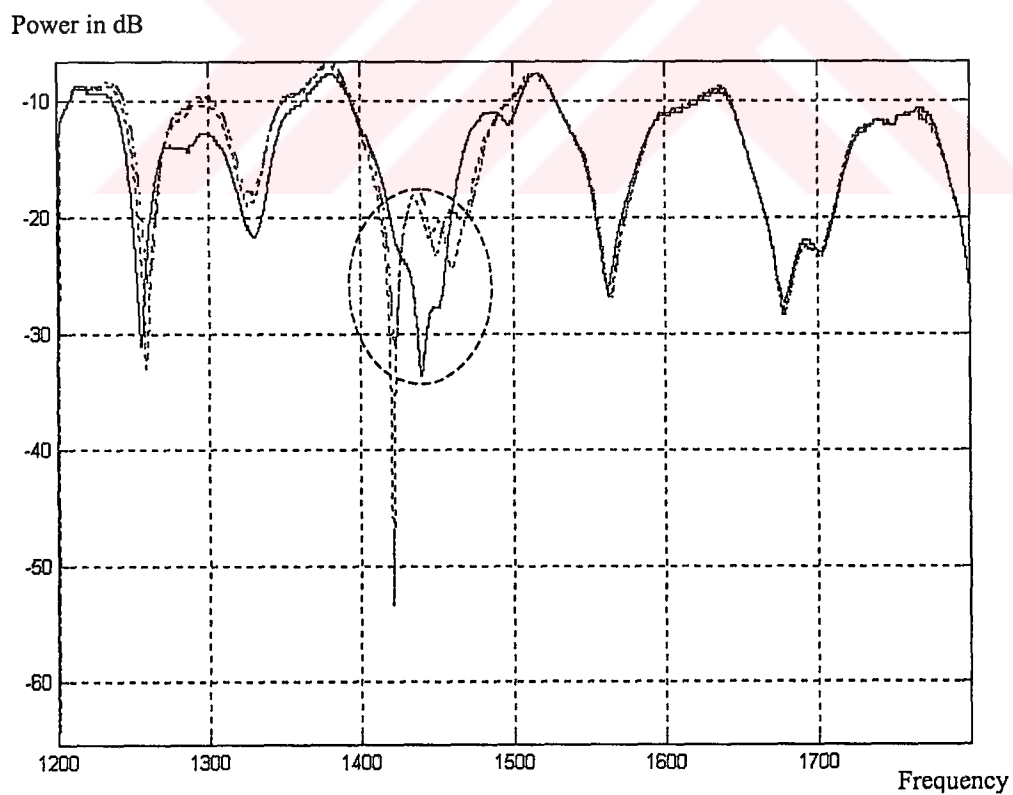


**Figure 3-22 Effect of changing red colored phase shifter voltage  
on Return loss**

As we can see from the graphs input impedance shows a perfect match at frequencies near 1450 MHz. This means that most of the power is absorbed from the feed line but radiation characteristics shows us that no radiation occurs at 1450 MHz. Thus we can say that power at 1450 MHz is absorbed by the phase shifter circuitry. Frequency response of the array is seen in Figure 3-23.

Power in dB

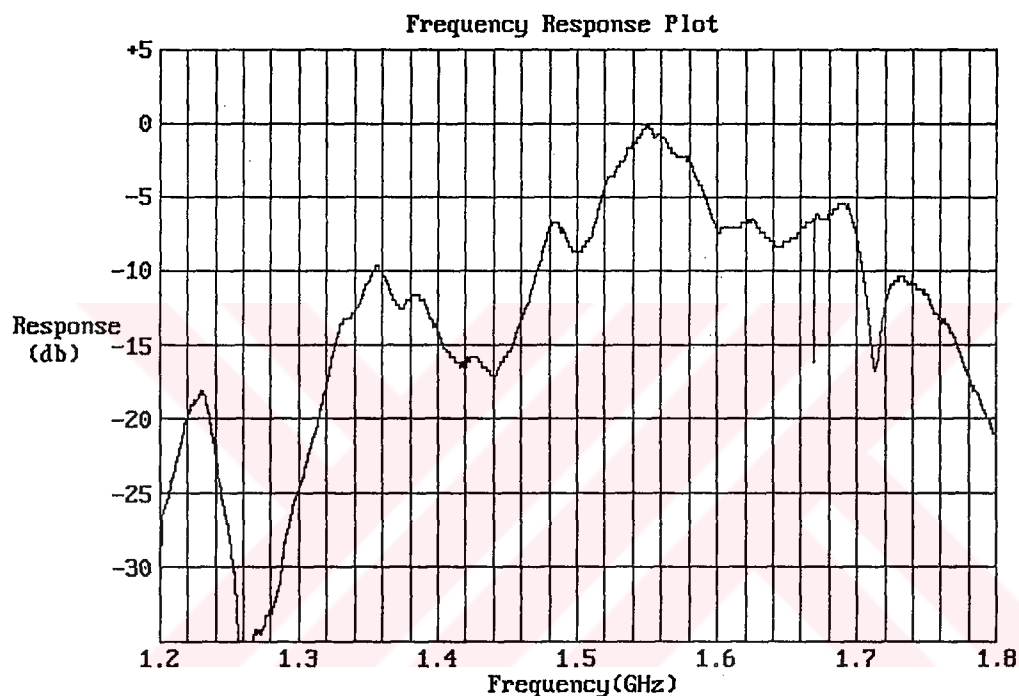


**Figure 3-23 Transmission response of the phase array antenna**

When we observe polar plot diagrams of the antenna we can observe that beam shifting occurs also at 1570 MHz. Polar plots for different bias voltages applied to phase shifters are given in below Figures 3-24 - 3-30. Antenna radiation pattern with equal phases can be seen in Figure 3-11

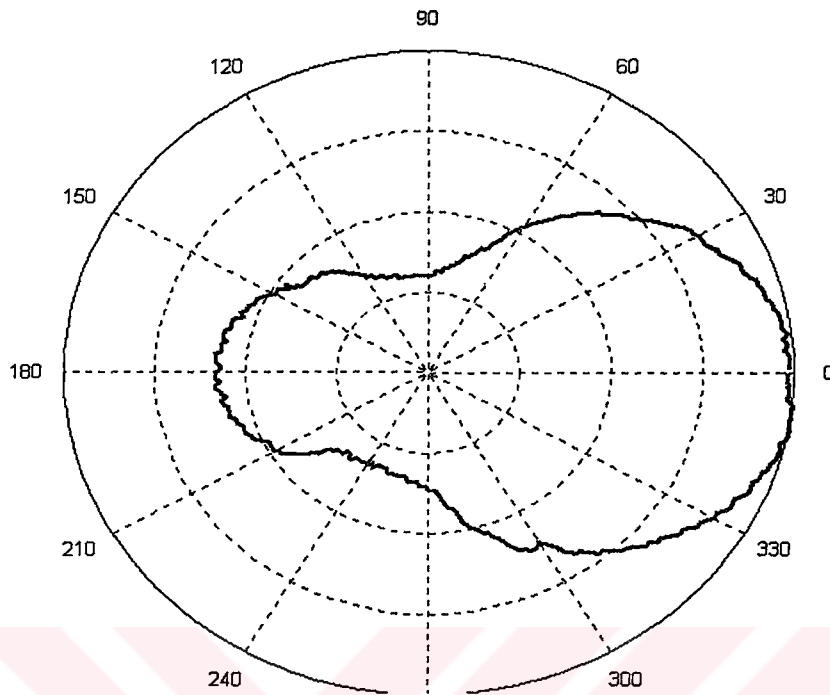


Figure 3-24 Radiation pattern of the phased array antenna with  $V_{bs}=16.5$  V

$V_{bn}=16$  V

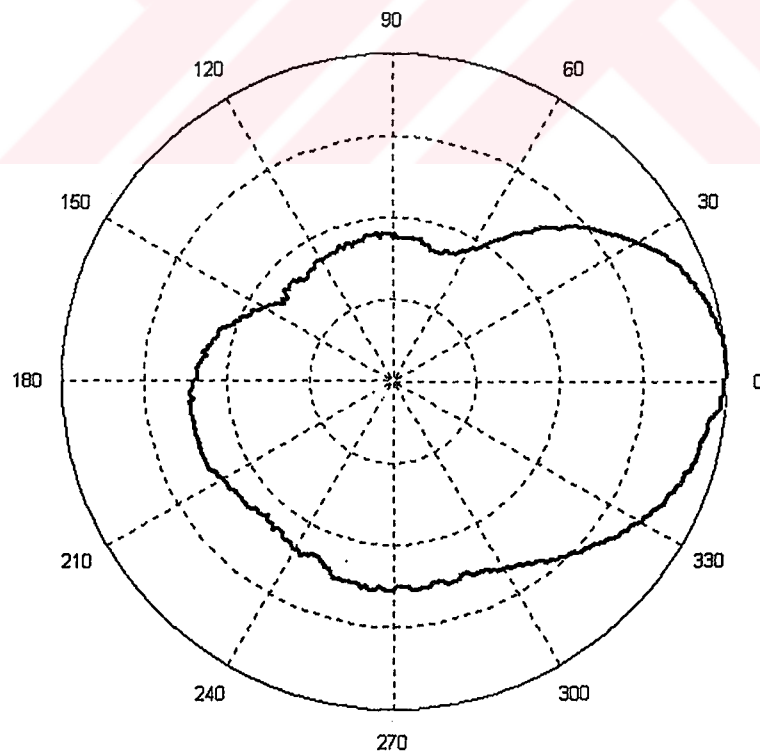
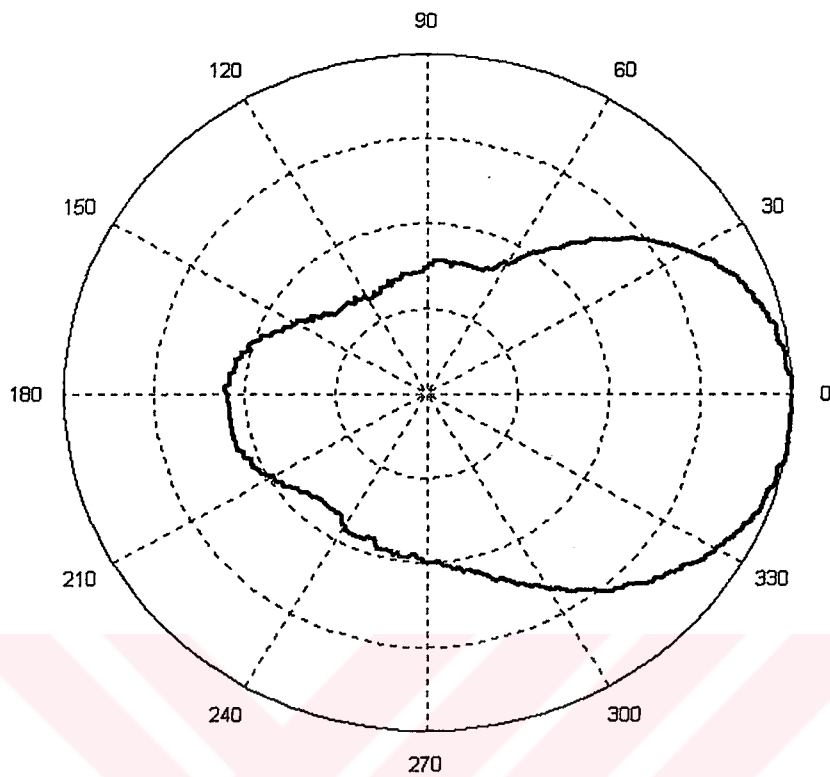


Figure 3-25 Radiation pattern of the phased array antenna with  $V_{bs}=19$  V

$V_{bn}=16$  V





**Figure 3-26 Radiation pattern of the phased array antenna with  $V_{bs}=25$  V  
 $V_{bn}=16$  V**

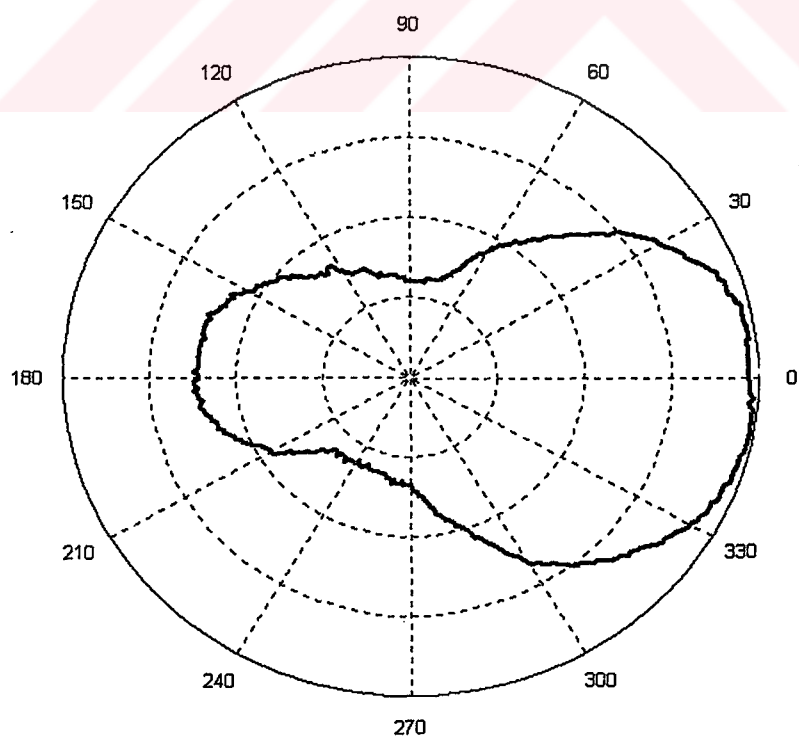


**Figure 3-27 Radiation pattern of the phased array antenna with  $V_{bs}=16$  V  
 $V_{bn}=22$  V**

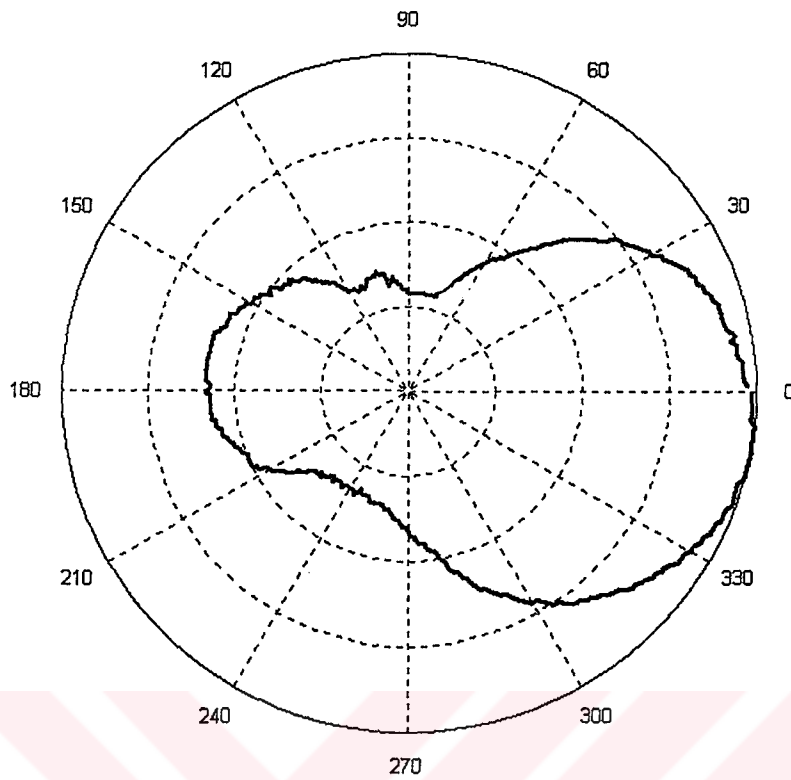


**Figure 3-28 Radiation pattern of the phased array antenna with  $V_{bs}=16$  V  
 $V_{bn}=24$  V**

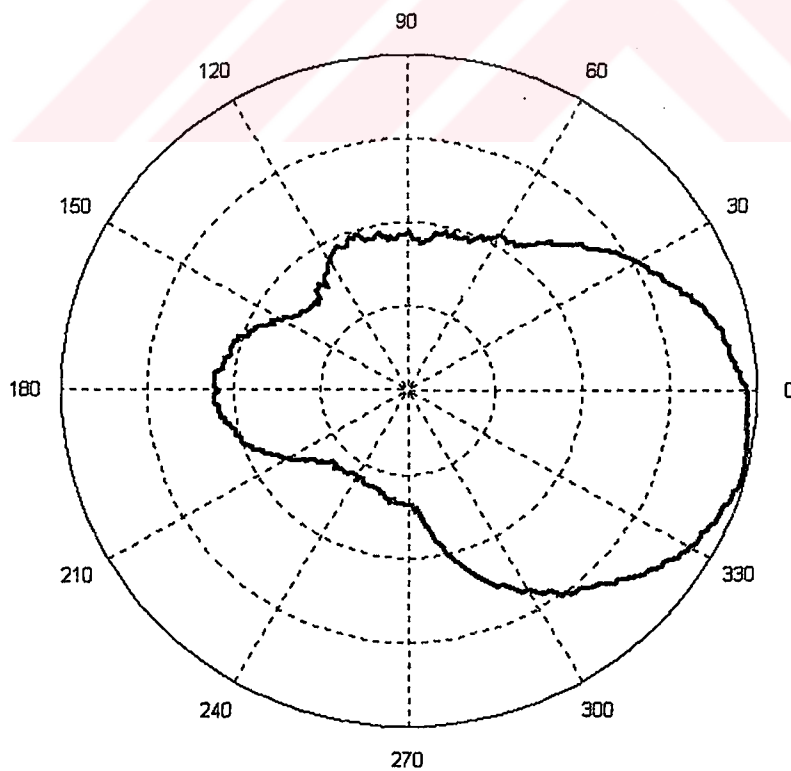


**Figure 3-29 Radiation pattern of the phased array antenna with  $V_{bs}=16$  V  
 $V_{bn}=27$  V**

From Figures 3-24 to 3-26 we can see that by increasing the silver painted phase shifter beam can be shifted 15 degrees in positive direction and from Figures 3-27 to 3-29 antenna beam is shifted 15 degrees in negative direction by controlling the bias voltage of the non colored phase shifter.

Thus we can see that by controlling the bias voltages we can steer the beam of the antenna a total of 30 degrees. This means a total phase shift of nearly 90 degrees.

This phase shift occurs because of radiation frequency of the antenna is slightly out of range of the phase shifters. They both can be put in the same range by slightly tuning the phase shifters especially by changing the DC block capacitors.



---

## CHAPTER FOUR

# CONCLUSION AND FUTUREWORK

---

In this thesis an antenna for mobile satellite communications is designed and realized. A suitable antenna type is considered as aperture coupled microstrip phased array antenna. Design steps and implementation of this antenna can be seen step by step in chapter three.

### 4.1 Comments on Antenna Performance

As a first step a circular microstrip antenna was designed to operate at 1550 MHz which is also a preferred band for land mobile satellite systems. Feeding of the antenna is realized with aperture coupled feeding in order to maximize the free area on the feed substrate for the phase shifting circuitry. This technique also increased our bandwidth and decreased feed line radiation which could corrupt our main lobe. Most important parameters of this technique is aperture size and tuning stub length which can be used to tune up the antenna to give maximum performance at desired frequency. Two different dielectric substrates were used in this single feed in order to find the suitable one. Comparison of return losses of antennas at same patches can be seen in Tables 3.2 and 3.2. A return loss of 17 dB can be reached by using GML1000 with dimensions of 2.4 in length and 2.5 mm width. As a result GML 1000 showed us a better performance even if thickness is more than the FR4. GML1000 is chosen for our feed layer substrate. Thus antenna is matched at operating frequency and has a wider bandwidth when compared with a contact fed MSA.

Observation of polar plots in E and H planes show us that antenna's back lobe radiation is negligibly small when compared to main lobe of the antenna. The E plane pattern for a typical MSA is smooth having a beam width of 100 degrees while H plane pattern goes to zero with smaller beam width (Schaubert 1995). Our antennas radiation characteristics match with these results as can be seen from Figures 3.1 and 3.2. Our antennas transmission characteristic is tested at a specified

distance with an identical one in order to derive its gain. From some calculations shown in chapter 3, gain is evaluated as 2.5 dB. These characteristics show us that our antenna is suitable for our application.

Next step is to implement the parameters evaluated from the design of a single antenna to the array. For simplicity and easy integrability a  $\lambda/2$  dual array antenna was designed. Values evaluated in testing of a single MSA are used in the dual array feed. A rise in operating frequency occurred in the array because feed layer effects mutual and coupling between antennas. Return loss of the array was also satisfactory and it had enough bandwidth. Directivity of the array is 3 times the directivity of the single antenna designed. Gain of the array is also computed like in a single antenna and it was found to be 8.57 dB and it is 3.5 times the gain of a single antenna.

This ratio for the gain can be thought as satisfactory when compared with a single antenna but we need better gain for a real operating satellite network. So we can say an array with more elements is needed. Tracking only E plane can be accomplished with our antenna but we should steer the beam in order to track the whole sky. This objective can be obtained by using two dimensional antenna arrays like planar or circular arrays

In order to step up to a phased array we need a suitable phase shifter which is defined in chapter 2. As can be seen in Figure 2-18 we can steer the beam of the antenna to 60 degrees to one side by shifting the relative phase between antennas 90 degrees. Steering the beam to  $\pm 60$  degrees. Thus this gives us a 120 degree beam steering option which is a satisfactory result for LMSS.

A suitable phase shifter was modeled by using APLAC student version 7.62 and results were considered with the implemented one by using spectrum analyzer. Magnitude graphs just fitted with the simulation which helped determining the phase shift which can not be observed with the spectrum analyzer. A phase shift of  $90^\circ$  can be evaluated by using this phase shifter with transmission loss of 1-1.5 dB.

In order to tune up the phase shifter to desired frequency very small DC blocking capacitors were used. This is because of the frequency dependence of the varicap diodes (MBV209 from On Semiconductors) used in the circuitry. It is originally designed for UHF band so values are optimized to work at a maximum of 800 MHz. Expected capacitance value at 1500MHz is very small when compared with values

given in data sheet (Appendix A). By using small DC blockage capacitors varicap capacitance value could be controlled in a meaningful area. This small DC blocking capacitors were evaluated by using 5mm x 5mm FR4 materials with calculated capacitance of 1 pF.

Applying this phase shifter on the dual feeds of the array antenna we got a phased array. Testing this array by changing the bias voltages of the varicaps we see that beam of the array is shifted towards the lower voltage level side. Phase shifters mounted on the array had a very narrow bandwidth. But they showed good performance at 1550 MHz.

Choosing varicaps to give equal capacitance value at same voltage makes our circuitry more reliable. Also microstrip capacitors can be designed to increase reliability as a futurework.

**Table 4.1 Comparison of resultant antennas performance values**

Antenna Type	Return Loss (dB)	Gain (dB)	Beamwidth (E plane)
Single Antenna	-21	5.6	90 <sup>0</sup>
Dual Antenna	-17	8.5	45 <sup>0</sup>
Phased Antenna	-13	7.5	45 <sup>0</sup>

#### 4.2 Futurework

A PC interface circuitry is to be designed to control the bias voltages of the varicaps. This could be accomplished through the parallel port of the PC by connecting DAC's to each data port. This would give us freedom to control the beam through an easy PC interface.

Future work on this thesis involves designing an array whose beam can be directed in a three dimensional space. This is preferably a planar array or a circular array. Even if beam directing logic is more complex in a circular array it is a preferable type of array because it is directed shape is thinner and side lobes are smaller.

Also the frequency response of the phase shifting network should be investigated over a wide frequency range.

---

## REFERENCES

---

Aksun M.I., (1991) Novel Feeds for Microstrip and Slot Antennas, Theory and Experiment pp 7-16

Balanis C.A.(1996). Antenna Theory (2<sup>nd</sup> ed.). Tempe AZ, John Wiley & Sons Inc

Bialkowski M.E., Karmakar N.C., (June 1999) A two ring circular polarized Phased- Array antenna. IEEE Antennas and Propagation Magazine pp 14-24.

Carver K.R., Mink J.W., (1981), Microstrip Antennas. In Pozar D.M., Schaubert D.H. (Eds), Microstrip Antenna Technology

Garver R.V. (1976). Microwave Diode Control Devices. Artech House Inc.

Himdi M., Daniel J.P., Terret C.,(1990), Microstrip Antennas. In Pozar D.M., Schaubert D.H. (Eds), Analysis of Aperture Coupled Microstrip Antennas Using Cavity Method

Ispir R., Nogi S., Sanagi M., Fukui K. (1997) Transmission line coupling of Active Microstrip antennas. IEICE Trans. Electron. Vol. E80 1211-1220

Karmakar N.C., Bialkowski M.E., (1999) Circularly Polarized Aperture Coupled Circular Microstrip Patch Antennas for L Band Applications. IEEE Trans. Antennas and Propagation Vol. 47 933-940

Ludwig R., Bretchko P., (1976). RF Circuit Design. Prentice Hall

Lo Y.T. (1987), Antenna Handbook. In Lo Y.T., Lee. S.W. (Eds), Array Theory

Munson R.E., (1974), Microstrip Antennas. In Pozar D.M., Schaubert D.H. (Eds), Conformal Microstrip Antennas and Microstrip Phased Arrays

Pozar D.M., (1992). Microstrip Antennas. Proceedings of the IEEE Vol 80 79-91

Pozar D.M. (1996) A review of Aperture Coupled Microstrip Antennas. Amherst

Schaubert D.H. ,(1995), Microstrip Antennas. In Pozar D.M., Schaubert D.H. (Eds), A Review of Some Microstrip Antenna Characteristics

Sorace R., (1999) Overview of Multiple Satellite Communication Networks. IEEE Trans. Aerospace and Electronic Systems vol. 35 1362-1368

Tang R. (1987), Antenna Handbook. In Lo Y.T., Lee. S.W. (Eds), Practical Aspects of Phased Array Design

Targonski S.D., Pozar D.M. , (1985), Microstrip Antennas. In Pozar D.M., Schaubert D.H. (Eds), Design of Wideband Circularly Polarized Aperture Coupled Microstrip Antennas



# APPENDIX

## Datasheets Of Materials Used In The Thesis

### ON Semiconductor

## Silicon Epicap Diodes

Designed for general frequency control and tuning applications; providing solid-state reliability in replacement of mechanical tuning methods.

- High Q with Guaranteed Minimum Values at VHF Frequencies
- Controlled and Uniform Tuning Ratio
- Available in Surface Mount Package

#### MAXIMUM RATINGS

Rating	Symbol	MBV109T1	MMBV109LT1	MV209	Unit
Reverse Voltage	$V_R$	30			Vdc
Forward Current	$I_F$	200			mAdc
Forward Power Dissipation @ $T_A = 25^\circ\text{C}$ Derate above $25^\circ\text{C}$	$P_D$	280	200	200	mW
		2.8	2.0	1.6	mW/ $^\circ\text{C}$
Junction Temperature	$T_J$	+125			$^\circ\text{C}$
Storage Temperature Range	$T_{stg}$	-55 to +150			$^\circ\text{C}$

#### DEVICE MARKING

MBV109T1 = J4A, MMBV109LT1 = M4A, MV209 = MV209

#### ELECTRICAL CHARACTERISTICS ( $T_A = 25^\circ\text{C}$ unless otherwise noted.)

Characteristic	Symbol	Min	Typ	Max	Unit
Reverse Breakdown Voltage ( $I_R = 10 \mu\text{A}$ )	$V_{(BR)R}$	30	—	—	Vdc
Reverse Voltage Leakage Current ( $V_R = 25 \text{ Vdc}$ )	$I_R$	—	—	0.1	$\mu\text{A}$
Diode Capacitance Temperature Coefficient ( $V_R = 3.0 \text{ Vdc}$ , $f = 1.0 \text{ MHz}$ )	$TC_C$	—	300	—	ppm/ $^\circ\text{C}$

Device	$C_1$ , Diode Capacitance $V_R = 3.0 \text{ Vdc}$ , $f = 1.0 \text{ MHz}$ pF			Q, Figure of Merit $V_R = 3.0 \text{ Vdc}$ $f = 50 \text{ MHz}$	$C_R$ , Capacitance Ratio $C_3/C_{25}$ $f = 1.0 \text{ MHz}$ (Note 1)	
	Min	Nom	Max		Min	Max
MBV109T1, MMBV109LT1, MV209	26	29	32	200	5.0	6.5

1.  $C_R$  is the ratio of  $C_1$  measured at 3 Vdc divided by  $C_1$  measured at 25 Vdc.

MMBV109LT1 is also available in bulk packaging. Use MMBV109L as the device title to order this device in bulk.

**MBV109T1**  
**MMBV109LT1** \*  
**MV209** \*

\* ON Semiconductor Preferred Devices

26–32 pF  
VOLTAGE VARIABLE  
CAPACITANCE DIODES



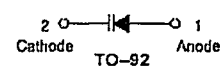
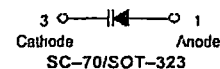
CASE 419-04, STYLE 3  
SC-70/SOT-323



CASE 318-08, STYLE 6  
SOT-23 (TO-236AB)



CASE 182-06, STYLE 1  
TO-92 (TO-226AC)



MBV109T1 MMBV109LT1 MV209

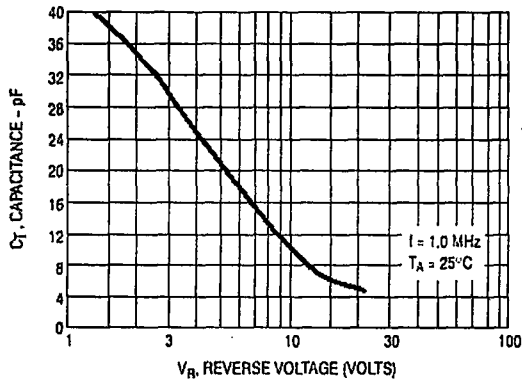


Figure 1. DIODE CAPACITANCE

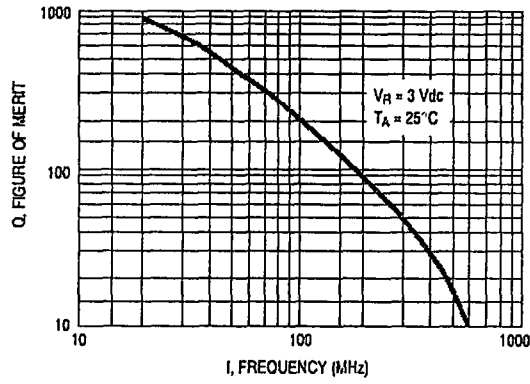


Figure 2. FIGURE OF MERIT

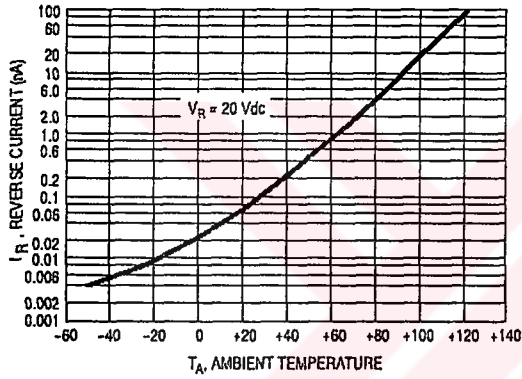


Figure 3. LEAKAGE CURRENT

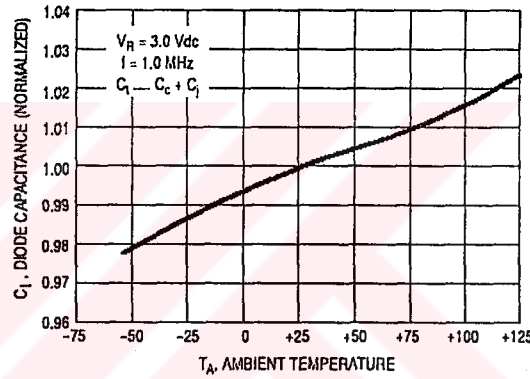


Figure 4. DIODE CAPACITANCE

NOTES ON TESTING AND SPECIFICATIONS

1.  $C_R$  is the ratio of  $C_T$  measured at 3.0 Vdc divided by  $C_T$  measured at 25 Vdc.

## GML 1000 High Frequency Laminate

(Typical Properties of 0.060 ±0.003 inch Thickness)



Electrical Properties	Frequency	Temperature		
		-55°C	25°C	80°C
Dielectric Constant per IPC-TM-650 2.5.5.5	2.5 GHz	3.05±.05	3.05±.05	3.05±.05
	10.0 GHz	3.05±.05	3.05±.05	3.05±.05
Dissipation Factor per IPC-TM-650 2.5.5.5	2.5 GHz	0.002	0.003	0.004
	10.0 GHz	0.003	0.004	0.005
dB/inch Loss (S <sub>21</sub> parameter from a 50 ohm 10 inch long transmission line)	1.0 GHz		0.023	
	5.0 GHz		0.123	
	10.0 GHz		0.295	
Surface Resistivity	C-96/35/90		Megohm	2 X 10 <sup>8</sup>
Volume Resistivity	C-96/35/90		Megohm-cm	8 X 10 <sup>8</sup>
Moisture Insulation Resistance	20 cycles -2°C/90% RH to 65°C/95% RH		Megohm	1 X 10 <sup>7</sup>
Solvent Extract Conductivity	-		µg/cm <sup>2</sup>	0.49

### Physical Properties

Copper peel strength (1 oz copper)	Condition A	Lb /inch width	5.0
	After 20 sec @550°F	Lb /inch width	5.0
Flexural Strength	Condition A	PSI	25,000
	Condition A	PSI	22,500
Flexural Modulus	Condition A	MPSI	1.6
	Condition A	MPSI	1.5
Moisture Absorption	D-24/23	%	0.02

### Thermal Properties

Glass Transition Temperature (DMA)	Condition A	°C	135
Thermal Stress	@550°F	seconds	20+
Z-Axis Expansion RT → T <sub>g</sub>	Condition A	ppm/°C	80
Z-Axis Expansion T <sub>g</sub> → 260°C	Condition A	ppm/°C	410
X/Y Axis Expansion	Condition A	ppm/°C	40 / 34
Thermal Conductivity	@120°C	W/mK	0.170
Dimensional Stability	Length	E-4/105 + E-2/150	inch/inch
	Cross	E-4/105 + E-2/150	inch/inch

### Description

GIL Technologies new GML 1000 copper clad laminate has been specifically designed for the High Frequency Microstrip Antenna and Wireless Communications Market. GML 1000's dielectric constant (Dk) is low and stable when used over broad temperature and humidity operating ranges. The low insertion loss makes GML 1000 the most cost effective option when compared to PTFE and other recognized microwave laminates.

### Features and Benefits

- Dk stable -55°C to 125°C
- Dk stable in humid and dry environments
- UL 94 V-0 Approved.  
File #E87492 (Oxygen Index >40%)
- No special through-hole treatments
- Fabrication and assembly in standard PWB operations
- Standard FR4 feeds & speeds for drilling & routing
- Excellent mechanical and electrical properties
- Absolutely the BEST cost performance available

- Typical properties of 0.060" laminate clad with 1 ounce copper.  
Properties of other thicknesses and copper weights may vary.